radiation therapy resulted in a significant improvement in local control and survival compared with radiation therapy alone, without an increase in radiation-induced side effects, in patients with locally advanced head and neck cancer (Bonner *et al*, 2006).

Nimotuzumab (also known as h-R3) is a humanised anti-EGFR mAb, which is currently undergoing clinical evaluation. In a preclinical study, nimotuzumab showed marked antiproliferative, proapoptotic, and antiangiogenic effects in tumours that overexpress EGFR (Crombet-Ramos *et al*, 2002). In early clinical trials, nimotuzumab has shown a longer half-life and a greater area under the curve (AUC) in comparison with other anti-EGFR antibodies (Crombet *et al*, 2003). A phase I/II trial showed that nimotuzumab was well tolerated and enhanced the curative potential of radiation in patients with advanced head and neck cancer (Crombet *et al*, 2004). Given that little is known of the antitumor action of nimotuzumab in NSCLC, we investigated the growth-inhibitory effects of this mAb alone and in combination with radiation in NSCLC cell lines with differing patterns of EGFR expression. We also examined whether genetic alterations of *EGFR* affect the antitumor action of combined treatment with nimotuzumab and radiation.

Translational Therapeutics

MATERIALS AND METHODS

Cell lines and reagents

The human NSCLC cell lines NCI-H292 (H292), NCI-H460 (H460), Ma-1, NCI-H1299 (H1299), and NCI-H1975 (H1975) were obtained as previously described (Okabe *et al*, 2007) and were maintained under a humidified atmosphere of 5% CO_2 in air at 37.0°C in RPMI 1640 medium (Sigma, St Louis, MO, USA) supplemented with 10% fetal bovine serum and 1% penicillin–streptomycin. Nimotuzumab was provided by Daiichi Sankyo Co Ltd (Tokyo, Japan), and gefitinib was obtained from AstraZeneca (Macclesfield, UK).

Flow cytometric analysis of surface EGFR expression

Cells (1.0×10^6) were stained for 2 h at 4°C with an R-phycoerythrin-conjugated mAb to EGFR (BD Biosciences, San Jose, CA, USA) or an isotype-matched control mAb (BD Biosciences). The cells were washed three times before measurement of fluorescence with a flow cytometer (FACScalibur; Becton Dickinson, San Jose, CA, USA).

Immunoblot analysis

Cell lysates were fractionated by SDS-polyacrylamide gel electrophoresis on a 7.5% gel, and the separated proteins were transferred to a nitrocellulose membrane. After blocking of nonspecific sites, the membrane was incubated consecutively with primary and secondary antibodies, and immune complexes were detected with the use of enhanced chemiluminescence reagents, as described previously (Okabe *et al*, 2007). Primary antibodies to phosphorylated EGFR (pY1068) were obtained from Cell Signaling Technology (Beverly, MA, USA), and those to EGFR were from Zymed (South San Francisco, CA, USA). Horseradish peroxidase-conjugated goat secondary antibodies were obtained from Amersham Biosciences (Little Chalfont, UK).

Clonogenic assay

Exponentially growing cells in 25-cm^2 flasks were harvested by exposure to trypsin and counted. They were diluted serially to appropriate densities and plated in triplicate in 25-cm^2 flasks containing 10 ml of medium supplemented with 1% fetal bovine serum in the absence or presence of 700 nM nimotuzumab. After incubation for 24 h, the cells were exposed to various doses of γ-radiation with a ^{60}Co irradiator at a rate of approximately 0.82 Gy min^{-1} and at room temperature. The cells were then washed with phosphate-buffered saline, cultured in drug-free medium for 10–14 days, fixed with methanol : acetic acid (10 : 1, v/v), and stained with crystal violet. Colonies containing >50 cells were counted. The surviving fraction was calculated as (mean number of colonies)/(number of inoculated cells × plating efficiency). Plating efficiency was defined as the mean number of colonies divided by the number of inoculated cells for control cultures not exposed to nimotuzumab or radiation. The surviving fraction for combined treatment was corrected by that for nimotuzumab treatment alone. The dose enhancement factor was then calculated as the dose (Gy) of radiation that yielded a surviving fraction of 0.5 for vehicle-treated cells divided by that for nimotuzumab-treated cells (after correction for drug toxicity).

Antitumor activity of nimotuzumab with or without radiation *in vivo*

Animal experiments were performed in accordance with the Recommendations for Handling of Laboratory Animals for Biomedical Research, compiled by the Committee on Safety and Ethical Handling Regulations for Laboratory Animal Experiments, Kyoto University, and they met the requirements of the UKCCCR guidelines (Workman *et al*, 1998). Tumour cells (2×10^6) were injected subcutaneously into the right hind leg of 7-week-old female athymic nude mice. tumour volume was determined from caliper measurement of tumour length (L) and width (W) according to the formula $LW^2/2$. Treatment was initiated when tumours in each group achieved an average volume of approximately 170–200 mm^3. Treatment groups consisted of control, nimotuzumab alone, radiation alone, and the combination of nimotuzumab and radiation, with each group containing seven or eight mice. Nimotuzumab was administered intraperitoneally in a single dose of 1.0 mg per mouse; mice in the control and radiation-alone groups were injected with vehicle (physiological saline). Tumours in the right hind leg of mice were exposed to 10 Gy of γ-radiation with a ^{60}Co irradiator at a rate of approximately 0.32 Gy min^{-1} beginning 6 h after drug treatment. Growth delay (GD) was calculated as the time required for treated tumours to achieve a fivefold increase in volume minus the corresponding time required for control tumours. The enhancement factor was then determined as $(GD_{combination} - GD_{nimotuzumab})/(GD_{radiation})$.

RESULTS

Surface EGFR expression in NSCLC cell lines of differing *EGFR* status

We first examined the surface expression of EGFR in five NSCLC cell lines by flow cytometry. The *EGFR* status for the cell lines was determined in our previous study (Okabe *et al*, 2007). Three cell lines (H460, H292, and H1299) possess wild-type *EGFR* alleles, whereas the other two cell lines (Ma-1 and H1975) harbour *EGFR* mutations (Table 1). Ma-1 cells have an in-frame deletion in

Table 1 Characteristics of NSCLC cell lines

Cell line	EGFR surface expression	EGFR status
H460	Low	Wild type
H292	High	Wild type
H1299	Low	Wild type
Ma-1	Moderate	del(E746–A750)
H1975	Low	L858R/T790M

EGFR = epidermal growth factor receptor; NSCLC = non-small cell lung cancer

exon 19 (E746–A750). H1975 cells harbour the L858R mutation in exon 21 and a secondary mutation in exon 20 (T790M). Activating mutations in exons 19 and 21 are associated with sensitivity to EGFR-TKIs (Lynch *et al*, 2004; Paez *et al*, 2004; Pao *et al*, 2004; Cappuzzo *et al*, 2005; Mitsudomi *et al*, 2005; Takano *et al*, 2005), whereas the T790M mutation contributes to the development of resistance to these drugs (Kobayashi *et al*, 2005; Pao *et al*, 2005). Our flow cytometric analysis demonstrated that H292 and Ma-1 cells express high and moderate levels of EGFR on the cell surface, respectively, whereas H460, H1299, and H1975 cells showed a low level of surface EGFR expression (Figure 1).

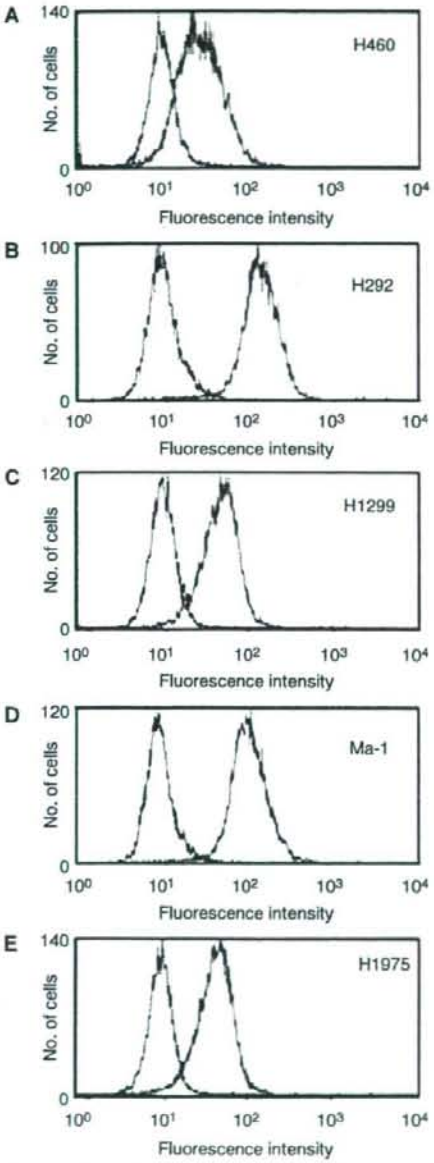

Figure 1 Expression of EGFR on the surface of NSCLC cells. Surface expression of EGFR on H460 (**A**), H292 (**B**), H1299 (**C**), Ma-1 (**D**), and H1975 (**E**) cells was determined by flow cytometry. Representative histograms of cells stained with an anti-EGFR mAb (red peak) or with an isotype-matched control mAb (black peak) are shown.

Effect of nimotuzumab on EGFR phosphorylation

Next, we determined whether nimotuzumab inhibits ligand-induced EGFR phosphorylation in the five NSCLC cell lines. The cells were deprived of serum overnight, exposed to various concentrations of nimotuzumab, or to gefitinib, for 15 min, and then stimulated with EGF for 15 min. In the NSCLC cells that harbour wild-type *EGFR* (H460, H292, and H1299), phosphorylation of EGFR was undetectable in the absence of EGF, but was markedly induced on exposure of the cells to this growth factor. The EGF-induced phosphorylation of EGFR in these cells was completely inhibited by the EGFR-TKI gefitinib. Nimotuzumab also inhibited the EGF-induced EGFR phosphorylation in a concentration-dependent manner in H292 cells (which have a high level of surface EGFR expression), whereas it did not substantially affect such phosphorylation in H460 or H1299 cells (both of which have a low level of surface EGFR expression) (Figure 2A–C). We previously showed that the basal level of EGFR phosphorylation was increased in the *EGFR* mutant NSCLC cell lines Ma-1 and H1975, indicative of constitutive activation of the EGFR tyrosine kinase (Okabe *et al*, 2007). The phosphorylation of EGFR in EGF-treated Ma-1 cells (which have a moderate level of surface EGFR expression) was inhibited by gefitinib as well as by nimotuzumab in a concentration-dependent manner (Figure 2D). In contrast, the constitutive activation of EGFR in H1975 cells (which have a low level of surface EGFR expression) was inhibited partially by gefitinib but was unaffected by nimotuzumab (Figure 2E). These results suggested that the inhibition of EGFR phosphorylation by nimotuzumab may be related to the surface expression level of EGFR rather than to the mutational status of *EGFR*.

Augmentation of the cytotoxic effect of radiation in NSCLC cells by nimotuzumab *in vitro*

We examined whether nimotuzumab might enhance the anticancer effect of γ-radiation in the five NSCLC cell lines with the use of a clonogenic assay. Tumour cells were incubated with or without nimotuzumab for 24 h, exposed to various doses of γ-radiation, and then allowed to form colonies in drug-free medium for 10–14 days. Survival curves revealed that, whereas nimotuzumab had no effect on the radiation sensitivity of H460, H1299, or H1975 cells, it enhanced the cytotoxic effect of radiation in H292 and Ma-1 cells, with a dose enhancement factor of 1.5 and 1.3, respectively (Figure 3). These results showed that nimotuzumab increased the radiosensitivity of the NSCLC cell lines with high or moderate levels of surface EGFR expression, consistent with the inhibitory effects of this antibody on EGFR signalling.

Augmentation of the antitumor effect of radiation in NSCLC cells by nimotuzumab *in vivo*

To determine whether the nimotuzumab-induced potentiation of the response of NSCLC cells to radiation observed *in vitro* might also be apparent *in vivo*, we injected three of the cell lines into nude mice to elicit the formation of solid tumours. The mice were then treated with nimotuzumab, radiation, or both modalities. In the H460 xenograft model, tumour growth was inhibited by radiation alone but not by nimotuzumab alone, and the effect of radiation was not promoted by nimotuzumab (Figure 4A). In contrast, radiation and nimotuzumab each inhibited the growth of tumours formed by H292 (Figure 4B) or Ma-1 (Figure 4C) cells during the first few weeks after treatment. Thereafter, the rate of

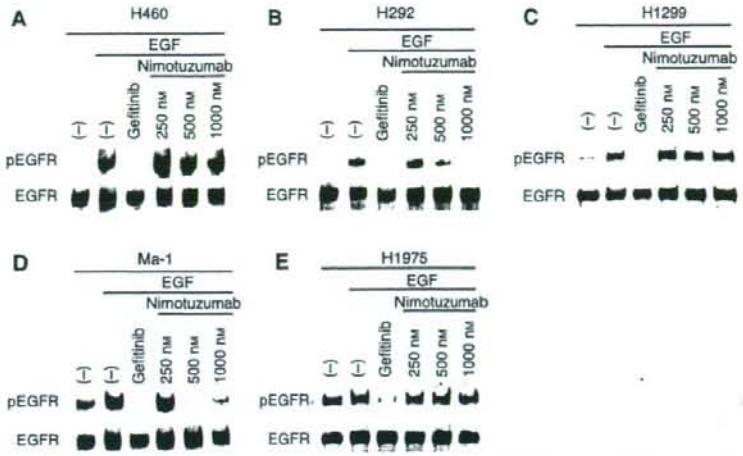

Figure 2 Effect of nimotuzumab on EGFR phosphorylation in NSCLC cells. H460 (**A**), H292 (**B**), H1299 (**C**), Ma-1 (**D**), and H1975 (**E**) cells were deprived of serum overnight and then incubated first for 15 min in the absence or presence of the indicated concentrations of nimotuzumab or gefitinib (10 μM) and then for an additional 15 min in the additional absence or presence of EGF (100 ng ml^{-1}). Cell lysates were then subjected to immunoblot analysis with antibodies to the Tyr1068-phosphorylated form of EGFR (pEGFR) as well as with those to total EGFR.

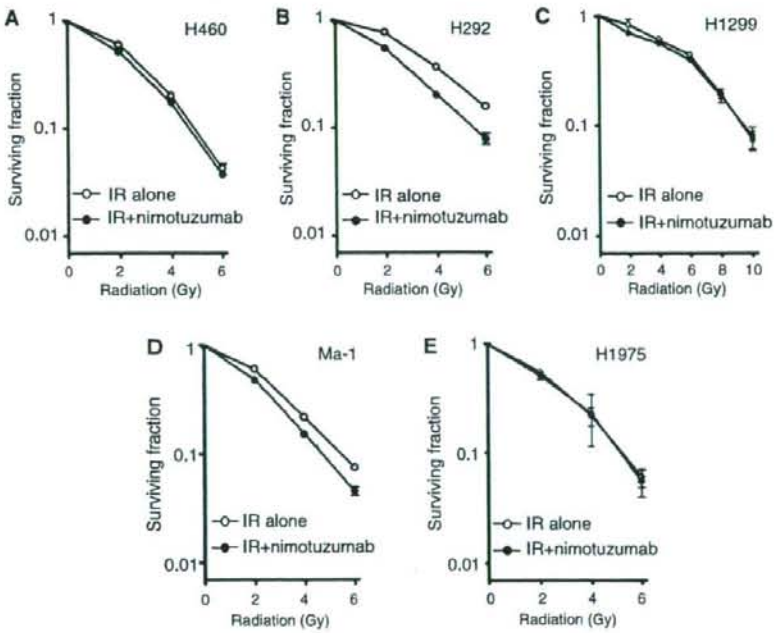

Figure 3 Effect of nimotuzumab on the response of NSCLC cells to radiation *in vitro*. H460 (**A**), H292 (**B**), H1299 (**C**), Ma-1 (**D**), and H1975 (**E**) cells were incubated with or without 700 nM nimotuzumab in medium supplemented with 1% fetal bovine serum for 24 h, exposed to the indicated doses of γ-radiation, and then incubated in drug-free medium supplemented with 10% serum for 10–14 days for determination of colony-forming ability. Survival curves were generated after correction of colony formation observed for combined treatment with ionising radiation (IR) and nimotuzumab by that apparent for treatment with nimotuzumab alone. Data are means ± s.d. of triplicates from a representative experiment.

tumour growth increased to a value similar to that seen in control animals. Combined treatment with radiation and nimotuzumab resulted in a substantial delay in tumour growth and subsequent inhibition of the growth rate of H292 and Ma-1 xenografts. The growth delay after treatment with nimotuzumab alone, radiation alone, or both nimotuzumab and radiation was thus 27.2, 19.6, and 53.6 days, respectively, for H292 cells and 26.7, 13.0, and 78.3 days, respectively, for Ma-1 cells (Table 2). The enhancement factor for the effect of nimotuzumab on the efficacy of radiation was 1.3 for H292 cells and 4.0 for Ma-1 cells, revealing the effect to be more

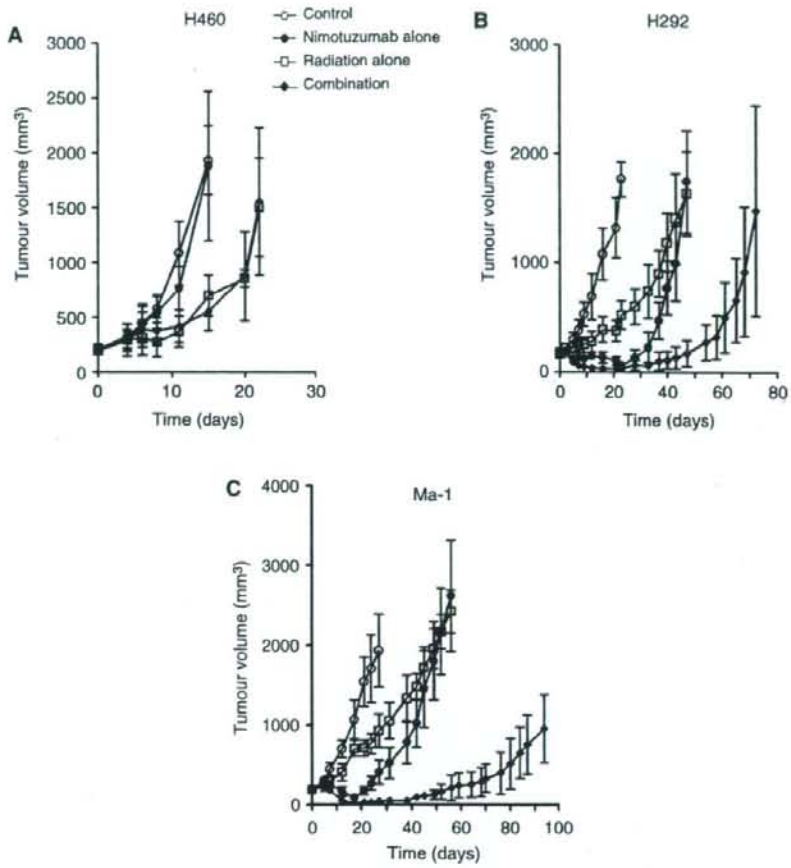

Figure 4 Effect of nimotuzumab on the response of NSCLC cells to radiation *in vivo*. H460 (**A**), H292 (**B**), or Ma-1 (**C**) cells were injected subcutaneously in athymic nude mice. Treatment was initiated when tumours in each group achieved an average volume of approximately 170–200 mm^3. Mice were treated with a single dose of nimotuzumab (1.0 mg per mouse) intraperitoneally, a single dose of γ-radiation (10 Gy), or neither (control) or both modalities, and tumour volume was determined at the indicated time points thereafter. Data are means ± s.d. for seven to eight mice per group.

Table 2 Tumour growth delay in nude mice treated with nimotuzumab, radiation, or both modalities

	H460		H292		Ma-1	
Treatment	**Days[a]**	**GD[b]**	**Days**	**GD**	**Days**	**GD**
Control	10.4		13.2		15.1	
Nimotuzumab alone	11.8	1.4	40.4	27.2	41.8	26.7
Radiation alone	20.4	10.0	32.8	19.6	28.1	13.0
Nimotuzumab+radiation	20.5	10.1	66.8	53.6	93.4	78.3
Enhancement factor	0.86		1.3		4.0	

GD = growth delay [a]Time required for xenografts in each group to achieve a fivefold increase in volume. [b]The additional time (days) required for xenografts in each treatment group to achieve a fivefold increase in volume relative to the corresponding time for xenografts in the control group.

than additive. No pronounced tissue damage or toxicities such as diarrhoea or a decrease in body weight of > 10% were observed in mice in any of the four treatment groups. These results thus suggested that nimotuzumab potentiated the antitumor activity of radiation in H292 and Ma-1 cells *in vivo* as well as *in vitro*.

DISCUSSION

Somatic mutations in the EGFR kinase domain and *EGFR* amplification have been associated with a better response to EGFR-TKIs, such as gefitinib and erlotinib, in patients with NSCLC (Lynch *et al*, 2004; Paez *et al*, 2004; Pao *et al*, 2004; Cappuzzo *et al*, 2005; Mitsudomi *et al*, 2005; Takano *et al*, 2005). Given that little is known of the relation between such *EGFR* alterations and the response to treatment with anti-EGFR mAbs, we investigated the antitumor effect of combined treatment with the anti-EGFR mAb nimotuzumab and radiation in NSCLC cell lines of differing *EGFR* status.

The antitumor effect of EGFR-specific mAbs has been thought to result from inhibition of ligand binding to EGFR and consequent inhibition of EGFR activation (Li *et al*, 2005; Marshall, 2006). We, therefore, examined the effect of nimotuzumab on EGF-dependent EGFR signalling. Nimotuzumab inhibited the EGF-induced or constitutive phosphorylation of EGFR in H292 and Ma-1 cells (with high and moderate levels of surface EGFR expression, respectively), consistent with the mode of action of this antibody. However, nimotuzumab did not block EGF-induced or constitutive EGFR phosphorylation in H460, H1299, or H1975 cells (all with a

low level of surface EGFR expression). These observations suggest that the inhibitory effect of nimotuzumab on EGFR signalling depends on the expression level of EGFR on the cell surface. A clonogenic cell survival assay revealed that nimotuzumab enhanced the cytotoxic effect of radiation in H292 and Ma-1 cells, but not that in H460, H1299, or H1975 cells. These findings support the notion that the inhibition of EGFR signalling by nimotuzumab is responsible, at least in part, for the enhancement of the cytotoxic effect of radiation by this antibody. Irradiation of tumour cells has been shown to activate EGFR via ligand-independent and ligand-dependent mechanisms, possibly accounting for radiation-induced acceleration of tumour cell repopulation and the development of radioresistance (Schmidt-Ullrich *et al*, 1997, 2003; Dent *et al*, 2003). Such radiation-induced activation of EGFR-dependent processes may represent a rationale for combined treatment with radiation and EGFR inhibitors. It remains to be determined whether nimotuzumab is able to block radiation-induced activation of EGFR.

Consistent with our *in vitro* results, we found that nimotuzumab enhanced the antitumor effect of radiation on H292 or Ma-1 cells in nude mice. Such enhancement was not apparent for tumours formed by H460 cells. Nimotuzumab alone also manifested a substantial antitumor effect for xenografts formed by H292 or Ma-1 cells but not for those formed by H460 cells. Together these results suggest that the efficacy of nimotuzumab monotherapy is a prerequisite for augmentation of radioresponse by this mAb. Nimotuzumab was previously shown to induce the regression of A431 tumour xenografts *in vivo* as a result of inhibition of both tumour cell proliferation and tumour angiogenesis (Crombet-Ramos *et al*, 2002). Immunohistochemical analysis of tumour specimens from head and neck cancer patients treated with the combination of nimotuzumab and radiation also showed evidence of antiproliferative and antiangiogenic effects (Crombet *et al*, 2004). These observations suggest that effects of nimotuzumab on both NSCLC cell proliferation and tumour angiogenesis might contribute to the enhancement of the antitumor efficacy of radiation by this antibody observed in the present study. Enhancement of the anticancer effect of radiation by the anti-EGFR mAb cetuximab was previously shown to be increased by transfection of cells to upregulate the level of EGFR expression, suggesting that potentiation of the antitumor efficacy of radiation by anti-EGFR mAbs is related to the absolute level of EGFR expression (Liang *et al*, 2003; Bonner *et al*, 2004). This finding is consistent with our present results showing that potentiation of the antitumor activity of radiation by nimotuzumab was related to the level of surface EGFR expression. The nimotuzumab-resistant cell line H460 harbours a mutant form of *KRAS* (Balko *et al*, 2006) that has been associated with resistance to cetuximab (Lievre *et al*, 2006). However, we found that nimotuzumab also failed to inhibit EGF-induced EGFR phosphorylation and to enhance the cytotoxic effect of radiation in H1299 cells, which harbour wild-type *KRAS* (Coldren *et al*, 2006). These observations thus support the notion that a low level of EGFR expression at the cell surface is related to resistance to combined treatment with nimotuzumab and radiation, irrespective of *KRAS* status.

We demonstrated that nimotuzumab inhibited EGFR phosphorylation and enhanced the antitumor effect of radiation in *EGFR* mutant Ma-1 cells (with a moderate level of surface EGFR expression) but not in *EGFR*-mutant H1975 cells (with a low level of surface EGFR expression). Nimotuzumab also potentiated the cytotoxic effect of radiation in H292 cells, which harbour wild-type *EGFR* alleles and have a high level of surface EGFR expression. These findings support the notion that *EGFR* mutation is not the major determining factor for enhancement of the antitumor effect of radiation by nimotuzumab, consistent with previous observations with cetuximab (Barber *et al*, 2004; Tsuchihashi *et al*, 2005). However, the mechanisms underlying such enhancement of the antitumor effect of radiation may differ between NSCLC cells harbouring wild-type or mutant *EGFR* alleles. We and others have previously shown that mutations in the tyrosine kinase domain of EGFR are associated with increased ligand-independent tyrosine kinase activity of EGFR (Lynch *et al*, 2004) and aberrant EGFR signalling (Amann *et al*, 2005; Okabe *et al*, 2007). Given that cell-cycle checkpoints activated by ionising radiation are defective in *EGFR*-mutant NSCLC cell lines (Das *et al*, 2006), the constitutive activity of EGFR in such cells may result in unchecked DNA synthesis and in apoptosis on exposure to ionising radiation. It is possible that these defects in *EGFR*-mutant cells affect the enhancement of the antitumor efficacy of radiation by nimotuzumab.

In summary, we have shown that nimotuzumab enhanced the antitumor efficacy of radiation *in vitro* and *in vivo*, providing a rationale for future clinical investigations of the therapeutic efficacy of nimotuzumab in combination with radiotherapy. Our data suggest that potentiation of the antitumor activity of radiation by nimotuzumab may be related to the level of EGFR expression at the cell surface rather than to *EGFR* mutation. The preselection of patients on the basis of genetic factors that predict treatment sensitivity or resistance may thus be required for the combination therapy with nimotuzumab and radiation.

ACKNOWLEDGEMENTS

We thank S Ono for technical assistance.

REFERENCES

Amann J, Kalyankrishna S, Massion PP, Ohm JE, Girard L, Shigematsu H, Peyton M, Juroske D, Huang Y, Stuart Salmon J, Kim YH, Pollack JR, Yanagisawa K, Gazdar A, Minna JD, Kurie JM, Carbone DP (2005) Aberrant epidermal growth factor receptor signaling and enhanced sensitivity to EGFR inhibitors in lung cancer. *Cancer Res* **65**: 226–235

Balko JM, Potti A, Saunders C, Stromberg A, Haura EB, Black EP (2006) Gene expression patterns that predict sensitivity to epidermal growth factor receptor tyrosine kinase inhibitors in lung cancer cell lines and human lung tumors. *BMC Genomics* **7**: 289

Barber TD, Vogelstein B, Kinzler KW, Velculescu VE (2004) Somatic mutations of EGFR in colorectal cancers and glioblastomas. *N Engl J Med* **351**: 2883

Baselga J (2002) Why the epidermal growth factor receptor? The rationale for cancer therapy. *Oncologist* **7**(Suppl 4): 2–8

Baselga J, Arteaga CL (2005) Critical update and emerging trends in epidermal growth factor receptor targeting in cancer. *J Clin Oncol* **23**: 2445–2459

Baumann M, Krause M (2004) Targeting the epidermal growth factor receptor in radiotherapy: radiobiological mechanisms, preclinical and clinical results. *Radiother Oncol* **72**: 257–266

Bonner JA, Buchsbaum DJ, Russo SM, Fiveash JB, Trummell HQ, Curiel DT, Raisch KP (2004) Anti-EGFR-mediated radiosensitization as a result of augmented EGFR expression. *Int J Radiat Oncol Biol Phys* **59**: 2–10

Bonner JA, Harari PM, Giralt J, Azarnia N, Shin DM, Cohen RB, Jones CU, Sur R, Raben D, Jassem J, Ove R, Kies MS, Baselga J, Youssoufian H, Amellal N, Rowinsky EK, Ang KK (2006) Radiotherapy plus cetuximab for squamous-cell carcinoma of the head and neck. *N Engl J Med* **354**: 567–578

Buchsbaum DJ, Bonner JA, Grizzle WE, Stackhouse MA, Carpenter M, Hicklin DJ, Bohlen P, Raisch KP (2002) Treatment of pancreatic cancer xenografts with Erbitux (IMC-C225) anti-EGFR antibody, gemcitabine, and radiation. *Int J Radiat Oncol Biol Phys* **54**: 1180–1193

Cappuzzo F, Hirsch FR, Rossi E, Bartolini S, Ceresoli GL, Bemis L, Haney J, Witta S, Danenberg K, Domenichini I, Ludovini V, Magrini E, Gregorc V, Doglioni C, Sidoni A, Tonato M, Franklin WA, Crino L, Bunn Jr PA, Varella-Garcia M (2005) Epidermal growth factor receptor gene and protein and gefitinib sensitivity in non-small-cell lung cancer. *J Natl Cancer Inst* **97:** 643–655

Coldren CD, Helfrich BA, Witta SE, Sugita M, Lapadat R, Zeng C, Baron A, Franklin WA, Hirsch FR, Geraci MW, Bunn Jr PA (2006) Baseline gene expression predicts sensitivity to gefitinib in non-small cell lung cancer cell lines. *Mol Cancer Res* **4:** 521–528

Crombet T, Osorio M, Cruz T, Roca C, del Castillo R, Mon R, Iznaga-Escobar N, Figueredo R, Koropatnick J, Renginfo E, Fernandez E, Alvarez D, Torres O, Ramos M, Leonard I, Perez R, Lage A (2004) Use of the humanized anti-epidermal growth factor receptor monoclonal antibody h-R3 in combination with radiotherapy in the treatment of locally advanced head and neck cancer patients. *J Clin Oncol* **22:** 1646–1654

Crombet T, Torres L, Neninger E, Catala M, Solano ME, Perera A, Torres O, Iznaga N, Torres F, Perez R, Lage A (2003) Pharmacological evaluation of humanized anti-epidermal growth factor receptor, monoclonal antibody h-R3, in patients with advanced epithelial-derived cancer. *J Immunother* **26:** 139–148

Crombet-Ramos T, Rak J, Perez R, Viloria-Petit A (2002) Antiproliferative, antiangiogenic and proapoptotic activity of h-R3: a humanized anti-EGFR antibody. *Int J Cancer* **101:** 567–575

Das AK, Sato M, Story MD, Peyton M, Graves R, Redpath S, Girard L, Gazdar AF, Shay JW, Minna JD, Nirodi CS (2006) Non-small cell lung cancers with kinase domain mutations in the epidermal growth factor receptor are sensitive to ionizing radiation. *Cancer Res* **66:** 9601–9608

Dent P, Yacoub A, Contessa J, Caron R, Amorino G, Valerie K, Hagan MP, Grant S, Schmidt-Ullrich R (2003) Stress and radiation-induced activation of multiple intracellular signaling pathways. *Radiat Res* **159:** 283–300

Ettinger DS (2006) Clinical implications of EGFR expression in the development and progression of solid tumors: focus on non-small cell lung cancer. *Oncologist* **11:** 358–373

Gschwind A, Fischer OM, Ullrich A (2004) The discovery of receptor tyrosine kinases: targets for cancer therapy. *Nat Rev Cancer* **4:** 361–370

Harari PM, Huang S (2006) Radiation combined with EGFR signal inhibitors: head and neck cancer focus. *Semin Radiat Oncol* **16:** 38–44

Huang SM, Bock JM, Harari PM (1999) Epidermal growth factor receptor blockade with C225 modulates proliferation, apoptosis, and radiosensitivity in squamous cell carcinomas of the head and neck. *Cancer Res* **59:** 1935–1940

Imai K, Takaoka A (2006) Comparing antibody and small-molecule therapies for cancer. *Nat Rev Cancer* **6:** 714–727

Kobayashi S, Boggon TJ, Dayaram T, Janne PA, Kocher O, Meyerson M, Johnson BE, Eck MJ, Tenen DG, Halmos B (2005) EGFR mutation and resistance of non-small-cell lung cancer to gefitinib. *N Engl J Med* **352:** 786–792

Li S, Schmitz KR, Jeffrey PD, Wiltzius JJ, Kussie P, Ferguson KM (2005) Structural basis for inhibition of the epidermal growth factor receptor by cetuximab. *Cancer Cell* **7:** 301–311

Liang K, Ang KK, Milas L, Hunter N, Fan Z (2003) The epidermal growth factor receptor mediates radioresistance. *Int J Radiat Oncol Biol Phys* **57:** 246–254

Lievre A, Bachet JB, Le Corre D, Boige V, Landi B, Emile JF, Cote JF, Tomasic G, Penna C, Ducreux M, Rougier P, Penault-Llorca F, Laurent-Puig P (2006) KRAS mutation status is predictive of response to cetuximab therapy in colorectal cancer. *Cancer Res* **66:** 3992–3995

Lynch TJ, Bell DW, Sordella R, Gurubhagavatula S, Okimoto RA, Brannigan BW, Harris PL, Haserlat SM, Supko JG, Haluska FG, Louis DN, Christiani DC, Settleman J, Haber DA (2004) Activating mutations in the epidermal growth factor receptor underlying responsiveness of non-small-cell lung cancer to gefitinib. *N Engl J Med* **350:** 2129–2139

Marshall J (2006) Clinical implications of the mechanism of epidermal growth factor receptor inhibitors. *Cancer* **107:** 1207–1218

Milas L, Mason K, Hunter N, Petersen S, Yamakawa M, Ang K, Mendelsohn J, Fan Z (2000) *In vivo* enhancement of tumor radioresponse by C225 antiepidermal growth factor receptor antibody. *Clin Cancer Res* **6:** 701–708

Mitsudomi T, Kosaka T, Endoh H, Horio Y, Hida T, Mori S, Hatooka S, Shinoda M, Takahashi T, Yatabe Y (2005) Mutations of the epidermal growth factor receptor gene predict prolonged survival after gefitinib treatment in patients with non-small-cell lung cancer with postoperative recurrence. *J Clin Oncol* **23:** 2513–2520

Okabe T, Okamoto I, Tamura K, Terashima M, Yoshida T, Satoh T, Takada M, Fukuoka M, Nakagawa K (2007) Differential constitutive activation of the epidermal growth factor receptor in non-small cell lung cancer cells bearing EGFR gene mutation and amplification. *Cancer Res* **67:** 2046–2053

Paez JG, Janne PA, Lee JC, Tracy S, Greulich H, Gabriel S, Herman P, Kaye FJ, Lindeman N, Boggon TJ, Naoki K, Sasaki H, Fujii Y, Eck MJ, Sellers WR, Johnson BE, Meyerson M (2004) EGFR mutations in lung cancer: correlation with clinical response to gefitinib therapy. *Science* **304:** 1497–1500

Pao W, Miller V, Zakowski M, Doherty J, Politi K, Sarkaria I, Singh B, Heelan R, Rusch V, Fulton L, Mardis E, Kupfer D, Wilson R, Kris M, Varmus H (2004) EGF receptor gene mutations are common in lung cancers from 'never smokers' and are associated with sensitivity of tumors to gefitinib and erlotinib. *Proc Natl Acad Sci USA* **101:** 13306–13311

Pao W, Miller VA, Politi KA, Riely GJ, Somwar R, Zakowski MF, Kris MG, Varmus H (2005) Acquired resistance of lung adenocarcinomas to gefitinib or erlotinib is associated with a second mutation in the EGFR kinase domain. *PLoS Med* **2:** 225–235

Prewett MC, Hooper AT, Bassi R, Ellis LM, Waksal HW, Hicklin DJ (2002) Enhanced antitumor activity of anti-epidermal growth factor receptor monoclonal antibody IMC-C225 in combination with irinotecan (CPT-11) against human colorectal tumor xenografts. *Clin Cancer Res* **8:** 994–1003

Raben D, Helfrich B, Chan DC, Ciardiello F, Zhao L, Franklin W, Baron AE, Zeng C, Johnson TK, Bunn Jr PA (2005) The effects of cetuximab alone and in combination with radiation and/or chemotherapy in lung cancer. *Clin Cancer Res* **11:** 795–805

Schmidt-Ullrich RK, Contessa JN, Lammering G, Amorino G, Lin PS (2003) ERBB receptor tyrosine kinases and cellular radiation responses. *Oncogene* **22:** 5855–5865

Schmidt-Ullrich RK, Mikkelsen RB, Dent P, Todd DG, Valerie K, Kavanagh BD, Contessa JN, Rorrer WK, Chen PB (1997) Radiation-induced proliferation of the human A431 squamous carcinoma cells is dependent on EGFR tyrosine phosphorylation. *Oncogene* **15:** 1191–1197

Takano T, Ohe Y, Sakamoto H, Tsuta K, Matsuno Y, Tateishi U, Yamamoto S, Nokihara H, Yamamoto N, Sekine I, Kunitoh H, Shibata T, Sakiyama T, Yoshida T, Tamura T (2005) Epidermal growth factor receptor gene mutations and increased copy numbers predict gefitinib sensitivity in patients with recurrent non-small-cell lung cancer. *J Clin Oncol* **23:** 6829–6837

Tsuchihashi Z, Khambata-Ford S, Hanna N, Janne PA (2005) Responsiveness to cetuximab without mutations in EGFR. *N Engl J Med* **353:** 208–209

Workman P, Twentyman P, Balkwill F, Balmain A, Chaplin D, Double J, Embleton J, Newell D, Raymond R, Stables J, Stephens T, Wallace J (1998) United Kingdom Co-ordinating Committee on Cancer Research (UKCCCR) Guidelines for the Welfare of Animals in Experimental Neoplasia 2nd edn. *Br J Cancer* **77:** 1–10

Radiosensitizing Effect of YM155, a Novel Small-Molecule Survivin Suppressant, in Non–Small Cell Lung Cancer Cell Lines

Tsutomu Iwasa,[1] Isamu Okamoto,[1] Minoru Suzuki,[2] Takahito Nakahara,[4] Kentaro Yamanaka,[4] Erina Hatashita,[1] Yuki Yamada,[1] Masahiro Fukuoka,[3] Koji Ono,[2] and Kazuhiko Nakagawa[1]

Abstract

Purpose: Survivin, a member of the inhibitor of apoptosis protein family, is an attractive target for cancer therapy. We have now investigated the effect of YM155, a small-molecule inhibitor of survivin expression, on the sensitivity of human non–small cell lung cancer (NSCLC) cell lines to γ-radiation.

Experimental Design: The radiosensitizing effect of YM155 was evaluated on the basis of cell death, clonogenic survival, and progression of tumor xenografts. Radiation-induced DNA damage was evaluated on the basis of histone H2AX phosphorylation and foci formation.

Results: YM155 induced down-regulation of survivin expression in NSCLC cells in a concentration- and time-dependent manner. A clonogenic survival assay revealed that YM155 increased the sensitivity of NSCLC cells to γ-radiation *in vitro*. The combination of YM155 and γ-radiation induced synergistic increases both in the number of apoptotic cells and in the activity of caspase-3. Immunofluorescence analysis of histone γ-H2AX also showed that YM155 delayed the repair of radiation-induced double-strand breaks in nuclear DNA. Finally, combination therapy with YM155 and γ-radiation delayed the growth of NSCLC tumor xenografts in nude mice to a greater extent than did either treatment modality alone.

Conclusions: These results suggest that YM155 sensitizes NSCLC cells to radiation both *in vitro* and *in vivo*, and that this effect of YM155 is likely attributable, at least in part, to the inhibition of DNA repair and enhancement of apoptosis that result from the down-regulation of survivin expression. Combined treatment with YM155 and radiation warrants investigation in clinical trials as a potential anticancer strategy.

Survivin is a 16.5-kDa member of the inhibitor of apoptosis protein (IAP) family. It blocks the mitochondrial pathway of apoptosis by inhibiting caspases (1, 2) and regulates cell division through interaction with the proteins INCENP and Aurora B (3). It is abundant in many types of cancer cells but not in the corresponding normal cells (4–6). High levels of survivin expression in cancer cells are associated with poor patient prognosis and survival as well as with resistance to therapy and an increased rate of cancer recurrence (7–9). Survivin has therefore become a therapeutic target and potentially important prognostic marker for many tumor types, including non–small cell lung cancer (NSCLC; refs. 7, 10). Molecular antagonists of survivin including antisense oligonucleotides, and dominant negative mutants have been shown to induce apoptosis in cancer cells *in vitro* and *in vivo* as well as to enhance chemotherapy-induced cell death (11–13). Although antisense oligonucleotides and ribozymes can be engineered to be highly specific for survivin, they may be difficult to deliver in the clinical setting.

YM155, a small imidazolium-based compound, was identified by high-throughput screening of chemical libraries for inhibitors of the activity of the survivin gene promoter in a reporter assay (14). This compound specifically inhibits the expression of survivin at both the mRNA and protein levels and exhibits pronounced anticancer activity in preclinical models (14). An advantage of YM155 compared with previously investigated suppressors of survivin expression (15–20) is that it is active in the subnanomolar range. Pharmacokinetic analysis also revealed that YM155 was highly distributed to tumor tissue in tumor xenograft models *in vivo* (14). YM155 is thus an attractive candidate drug for cancer therapy, and clinical trials of YM155 in single-agent therapy are currently under way for some types of cancer.

Glioblastoma cells that overexpress survivin were found to be less responsive to radiation than survivin-negative cells in a preclinical model (21). Clinically, high levels of survivin expression have been associated with an increased risk of local treatment failure after radiochemotherapy in patients with rectal cancer (9). These observations suggest that survivin plays

Authors' Affiliations: [1]Department of Medical Oncology, Kinki University School of Medicine, Osaka-Sayama, Osaka, Japan; [2]Radiation Oncology Research Laboratory, Research Reactor Institute, Kyoto University, Sennan-gun, Osaka, Japan; and [3]Kinki University School of Medicine, Sakai Hospital, Minami-ku Sakai, Osaka, Japan; and [4]Institute for Drug Research, Astellas Pharma, Inc., Tsukuba-shi, Ibaraki, Japan

Received 2/20/08; revised 5/21/08; accepted 6/1/08.

The costs of publication of this article were defrayed in part by the payment of page charges. This article must therefore be hereby marked *advertisement* in accordance with 18 U.S.C. Section 1734 solely to indicate this fact.

Requests for reprints: Isamu Okamoto, Department of Medical Oncology, Kinki University School of Medicine, 377-2 Ohno-higashi, Osaka-Sayama, Osaka 589-8511, Japan. Phone: 81-72-366-0221; Fax: 81-72-360-5000; E-mail: chi-okamoto@dotd.med.kindai.ac.jp.

doi:10.1158/1078-0432.CCR-08-0468

Translational Relevance

Survivin is a potentially important molecular target for cancer therapy. Reflecting the many mechanisms that seem to regulate survivin expression, diverse approaches have been evaluated for targeting survivin in experimental models. YM155 is a novel small, imidazolium-based compound that specifically inhibits survivin expression in various types of cancer cell lines *in vitro*. In addition, YM155 has been shown to distribute preferentially to tumor tissues rather than to plasma as well as to exert pronounced antitumor activity in tumor xenograft models *in vivo*. The use of YM155 as a single agent in phase I clinical trials did not reveal significant toxicity. Although phase II studies of YM155 use as a single agent for certain types of cancer are currently under way, the effects of YM155 in combination with radiation have not been reported. We now show that inhibition of survivin expression by YM155 sensitizes tumor cells to radiation *in vitro* and *in vivo*. Therefore, our preclinical results provide a rationale for future clinical investigation of the therapeutic efficacy of YM155 in combination with radiotherapy.

a role in resistance to radiotherapy. Indeed, suppression of survivin expression with the use of antisense oligonucleotides or ribozymes has been shown to increase the radiosensitivity of cancer cells *in vitro* (20, 22–26). We have now examined the effects of the combination of YM155 and radiation on NSCLC cell lines *in vitro* and *in vivo*.

Materials and Methods

Cell culture and reagents. The human NSCLC cell lines NCI-H460 (H460) and Calu6 were obtained from the American Type Culture Collection. The cells were cultured under an atmosphere of 5% CO_2 at 37°C in RPMI 1640 (Sigma) supplemented with 10% fetal bovine serum. YM155 (Astellas Pharma, Inc.) was dissolved in DMSO.

Immunoblot analysis. Cells were washed twice with ice-cold PBS and then lysed in a solution containing 20 mmol/L Tris-HCl (pH 7.5), 150 mmol/L NaCl, 1 mmol/L EDTA, 1% Triton X-100, 2.5 mmol/L sodium PPi, 1 mmol/L phenylmethylsulfonyl fluoride, and leupeptin (1 μg/mL). The protein concentration of lysates was determined with the Bradford reagent (Bio-Rad), and equal amounts of protein were subjected to SDS-PAGE of a 15% gel. The separated proteins were transferred to a nitrocellulose membrane, which was then exposed to 5% nonfat dried milk in PBS for 1 h at room temperature before incubation overnight at 4°C with rabbit polyclonal antibodies to human survivin (1:1000 dilution; R&D Systems), to human c-IAP1 (1:1,000 dilution; MBL International), to human XIAP (1:1,000 dilution; Cell Signaling), to human STAT3 (1:1,000 dilution; Cell Signaling), or to β-actin (1:500 dilution; Sigma), or with mouse monoclonal antibodies to human p53 (1:1,000 dilution; Santa Cruz Biotechnology). The membrane was then washed with PBS containing 0.05% Tween 20 before incubation for 1 h at room temperature with horseradish peroxidase–conjugated goat antibodies to rabbit (Sigma) or mouse (Santa Cruz Biotechnology) IgG. Immune complexes were finally detected with chemiluminescence reagents (Perkin-Elmer Life Science).

Clonogenic survival assay. Exponentially growing cells in 25-cm^2 flasks were harvested by exposure to trypsin and counted. They were diluted serially to appropriate densities and plated in triplicate in 25-cm^2 flasks containing 10 mL of complete medium in the presence of 50 nmol/L YM155 or vehicle (final DMSO concentration of 0.1%; we confirmed that this DMSO concentration did not affect the proliferation of NSCLC cell lines). After incubation for 48 h, the cells were exposed at room temperature to various doses of γ-radiation with a ^{60}Co irradiator at a rate of −0.82 Gy/min. The cells were then washed with PBS, cultured in drug-free medium for 10 to 14 d, fixed with methanol:acetic acid (10:1, v/v), and stained with crystal violet. Colonies containing >50 cells were counted. The surviving fraction was calculated as: (mean number of colonies)/(number of inoculated cells × plating efficiency). Plating efficiency was defined as the mean number of colonies divided by the number of inoculated cells for nonirradiated control cells. The surviving fraction for combined treatment was corrected by that for YM155 treatment alone. Cell survival was corrected according to the equation $S = 1 - (1 - f)^{1/N}$, where S is the single-cell survival rate, f is the measured surviving fraction, and N is multiplicity, which was defined as the average number of cells per microcolony at the time of radiation and which ranged from 2.4 to 6.7 for the cell lines studied under the described conditions. The dose enhancement factor was then calculated as the dose (Gy) of radiation that yielded a surviving fraction of 0.1 for vehicle-treated cells divided by that for YM155-treated cells (after correction for drug toxicity).

Detection of apoptotic cells. Cells were fixed with 4% paraformaldehyde for 1 h at room temperature, after which a minimum of 1,000 cells per sample was evaluated for apoptosis with the use of the terminal deoxynucleotidyl transferase-mediated dUTP nick-end labeling (TUNEL) technique (*In situ* Cell Death Detection Kit; Boehringer Mannheim).

Assay of caspase-3 activity. The activity of caspase-3 in cell lysates was measured with the use of a CCP32/Caspase-3 Fluometric Protease Assay Kit (MBL). Fluorescence attributable to cleavage of the DEVD-AFC substrate was measured at excitation and emission wavelengths of 390 and 460 nm, respectively.

Immunofluorescence staining of γ-H2AX. Cells were grown to 50% confluence in two-well Lab-Tec Chamber Slides (Nunc) and then cultured for 48 h in the presence of 50 nmol/L YM155 or vehicle before exposure to 3 Gy of γ-radiation. At various times thereafter, they were fixed with 4% paraformaldehyde for 10 min at room temperature, permeabilized with 0.1% Triton X-100 for 10 min at 4°C, and exposed to 5% nonfat dried milk for 10 min at room temperature. The slides were washed with PBS and then incubated at room temperature first for 2 h with mouse monoclonal antibodies to histone γ-H2AX (Upstate Biotechnology) at a dilution of 1:300 and then for 1 h with Alexa 488–labeled goat antibodies to mouse IgG (Molecular Probes) at a dilution of 1:700. The slides were mounted in fluorescence mounting medium (Dako Cytomation), and fluorescence signals were visualized with a confocal laser-scanning microscope (Axiovert 200M; Carl Zeiss) equipped with the LSM5 PASCAL system (Carl Zeiss). Three random fields each containing ≈50 cells were examined at a magnification of × 100. Nuclei containing ≥10 immunoreactive foci were counted as positive for γ-H2AX, as previously described (27), and percentage of positive cells was calculated.

***Evaluation of tumor growth* in vivo.** All animal studies were done in accordance with the Recommendations for Handling of Laboratory Animals for Biomedical Research compiled by the Committee on Safety and Ethical Handling Regulations for Laboratory Animal Experiments, Kyoto University. The ethical procedures followed met the requirements of the United Kingdom Coordinating Committee on Cancer Research guidelines (28). Tumor cells (2×10^6) were injected s.c. into the right hind leg of 6-week-old female athymic nude mice (BALB/c nu/nu). Tumor volume was determined from caliper measurement of tumor length (L) and width (W) according to the formula $LW^2/2$. Treatment was initiated when the tumors in each group of animals achieved an average volume of ~200 to 250 mm^3. Treatment groups (each containing eight mice) consisted of vehicle control (physiologic saline), YM155 alone, vehicle plus radiation, and YM155 plus radiation. Vehicle or YM155 at a dose of 5 mg/kg of body mass was administered over 7 consecutive days (days 1-7) with the use of an implanted micro-osmotic pump (Alzet model 1003D; Durect). Mice in the radiation groups received 10 Gy of γ-radiation from a cobalt irradiator either as

a single fraction on day 3 of drug treatment or fractionated over 5 consecutive days (days 3 to 7); the radiation was targeted to the tumor, with the remainder of the body shielded with lead. Growth delay (GD) was calculated as the time required to achieve a 5-fold increase in volume for treated tumors minus that for control tumors. The enhancement factor was then determined as: $(GD_{combination} - GD_{YM155})/GD_{radiation}$.

Statistical analysis. Data are presented as means ± SD or SE and were compared with the unpaired Student's *t* test. A P value of <0.05 was considered statistically significant.

Results

Inhibition of survivin expression in NSCLC cells by YM155. We first examined the effect of YM155 on survivin expression in human NSCLC cell lines by immunoblot analysis. Treatment of H460 or Calu6 cells with YM155 at 1 to 100 nmol/L for 48 hours inhibited survivin expression in a concentration-dependent manner (Fig. 1A). In contrast, YM155 had no effect on the abundance of other members of the IAP family including XIAP and c-IAP1 (Fig. 1A), suggesting that YM155 specifically inhibits survivin expression in the NSCLC cell lines. The mechanism by which YM155 inhibits survivin expression remains to be elucidated. Previous observations have shown that p53 and signal transducer and activator of transcription 3 (STAT3) regulate survivin expression at the transcriptional level (29). We therefore examined the effect of YM155 on the abundance of p53 and STAT3 in NSCLC cell lines. YM155 showed no marked effect on the amounts of p53 and STAT3 in H460 or Calu6 cells (Fig. 1A), suggesting that the inhibition of survivin expression by YM155 is independent of these transcriptional regulators. Monitoring of the time course of survivin expression in cells exposed to 50 nmol/L

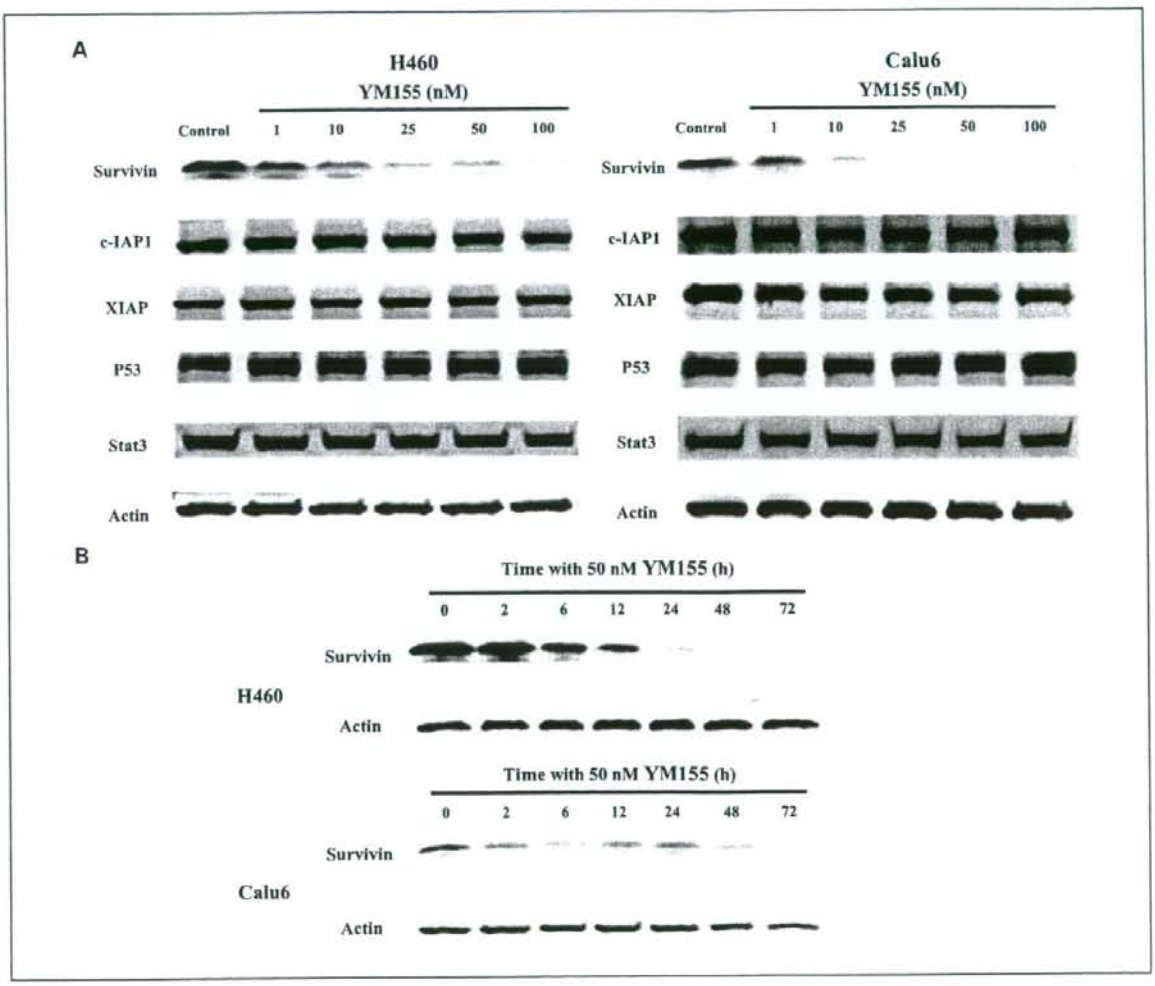

Fig. 1. Effect of YM155 on survivin expression in human NSCLC cells. *A*, H460 or Calu6 cells were incubated in the absence (control, 0.1% DMSO) or presence of various concentrations (1, 10, 25, 50, or 100 nmol/L) of YM155 for 48 h. Cell lysates were then prepared and subjected to immunoblot analysis with antibodies to survivin, to c-IAP1, to XIAP, to p53, to STAT3, or to β-actin (loading control). *B*, H460 or Calu6 cells were incubated with 50 nmol/L YM155 for the indicated times, after which cell lysates were subjected to immunoblot analysis with antibodies to survivin or to β-actin.

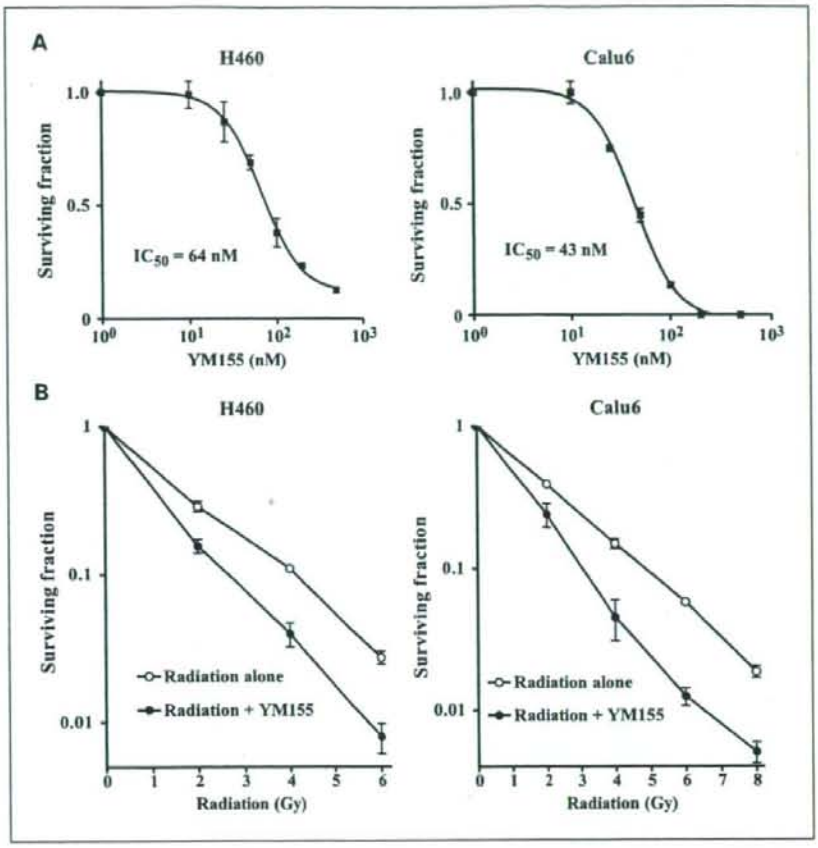

Fig. 2. Effect of YM155 on the sensitivity of H460 or Calu6 cells to γ-radiation. *A*, cells were incubated with the indicated concentrations of YM155 for 48 h and then assayed for clonogenic survival. Points represent means from three independent experiments; bars represent SD. *B*, cells were incubated with 50 nmol/L YM155 or vehicle (control, 0.1% DMSO) for 48 h, exposed to the indicated doses of γ-radiation, and then incubated in drug-free medium for 10 to 14 d for determination of colony-forming ability. Colonies were counted and the surviving fraction was calculated. Plating efficiency for nonirradiated H460 cells was 77.0% and 38.8% for vehicle-treated and YM155-treated cells, respectively; that for nonirradiated Calu6 cells was 57.0% and 23.5%, respectively. All surviving fractions with radiation were corrected for these baseline plating efficiencies. Points represent means from three independent experiments; bars represent SD.

YM155 for up to 72 hours revealed that the abundance of survivin in Calu6 cells had decreased by 2 hours and that survivin was virtually undetectable in H460 cells after 24 hours (Fig. 1B). In both cell lines, treatment with 50 nmol/L YM155 resulted in time-dependent inhibition of survivin expression.

YM155-induced sensitization of NSCLC cells to radiation. To examine the effect of YM155 on cell survival, we first did a clonogenic survival assay. Exposure to the drug at concentrations of 1 to 500 nmol/L for 48 hours revealed that YM155 inhibited the survival of H460 cells with a median inhibitory concentration (IC_{50}) of 64 nmol/L and that of Calu6 cells with an IC_{50} of 43 nmol/L (Fig. 2A). On the basis of these data, we adopted treatment with 50 nmol/L YM155 for 48 hours as the standard protocol for radiation experiments. We next examined whether YM155 might affect the sensitivity of NSCLC cell lines to radiation. Treatment with 50 nmol/L YM155 for 48 hours shifted the survival curves for both H460 and Calu6 cells to the left (Fig. 2B), with a dose enhancement factor of 1.57 and 1.61, respectively, suggesting that YM155 increased the radiosensitivity of both cell lines.

Enhancement of radiation-induced apoptosis in NSCLC cells by YM155. We next examined the effect of YM155 on radiation-induced apoptosis in H460 or Calu6 cells with the use of the TUNEL assay. Combined treatment of either cell line with YM155 and γ-radiation resulted in an increase in the number of apoptotic cells at 24 and 48 hours that was greater than the sum of the increases induced by YM155 or radiation alone (Fig. 3A). To confirm the results of the TUNEL assay, we measured the activity of caspase-3 in cell lysates. Again, the combined treatment of H460 or Calu6 cells with YM155 and γ-radiation induced a synergistic increase in caspase-3 activity (Fig. 3B). These data thus suggested that YM155 promotes radiation-induced apoptosis in NSCLC cell lines.

Inhibition of DNA repair in irradiated NSCLC cells by YM155. Defects in DNA repair have been associated with enhanced sensitivity of cells to radiation (30, 31), and survivin is thought to play a direct or indirect role in DNA repair (21). We therefore next investigated the effect of YM155 on DNA repair by immunostaining of cells with antibodies to the phosphorylated form (γ-H2AX) of histone H2AX, foci of which form at DNA double-strand breaks (DSBs). The formation of γ-H2AX foci in H460 cells was apparent between 30 minutes and 6 hours after γ-irradiation (Fig. 4A). In the presence of YM155, however, these foci persisted for at least 24 hours after irradiation. Evaluation of the percentage of H460 or Calu6 cells with γ-H2AX foci at 24 hours after irradiation revealed that YM155 significantly inhibited the repair of DSBs (Fig. 4B). These results thus suggested that down-regulation of survivin expression by YM155 results in the inhibition of the repair of

radiation-induced DSBs in NSCLC cells, possibly accounting for the observed radiosensitization by this drug.

Enhancement of radiation-induced tumor regression by YM155. To determine whether the YM155-induced radiosensitization of NSCLC cells observed *in vitro* might also be apparent *in vivo*, we injected H460 or Calu6 cells into nude mice to elicit the formation of solid tumors. After tumor formation, the mice were treated with YM155, γ-radiation, or both modalities. YM155 was infused continuously for 7 days with the use of an implanted osmotic pump system, and mice were subjected to local irradiation with a single dose of 10 Gy on day 3 of YM155 administration. Combined treatment with radiation and YM155 inhibited H460 or Calu6 tumor growth to a markedly greater extent than did either modality alone (Fig. 5). The tumor growth delays induced by treatment with radiation alone, YM155 alone, or both YM155 and radiation were 2.9, 5.6, and 14.8 days, respectively, for H460 cells, and 8.9, 41.0, and 76.0 days, respectively, for Calu6 cells. The enhancement factor for the effect of YM155 on the efficacy of radiation was 3.3 for H460 cells and 3.5 for Calu6 cells, revealing the effect to be greater than additive. No pronounced tissue damage or toxicity such as weight loss was observed in mice in any of the four treatment groups.

Finally, we evaluated whether the combination of YM155 and fractionated radiation treatment would result in the inhibition of tumor growth similar to that observed with YM155 plus single-fraction radiation. Mice bearing H460 tumors were thus again subjected to continuous YM155 infusion for 7 days, but local irradiation was done in 2-Gy fractions on days 3 to 7 of drug administration (for a total dose of 10 Gy). The tumor growth delays induced by treatment with radiation alone, YM155 alone, or both YM155 and radiation were 3.8, 5.3, and 16.6 days, respectively (Fig. 6). The enhancement factor for the effect of YM155 on the efficacy of radiation was 3.0. Again, there was no evidence of toxicity on the basis of body weight loss, and there were no animal deaths in any of the four groups. These data suggested that YM155 enhances the tumor response to both single-dose and fractionated radiotherapy *in vivo*.

Discussion

Survivin is a potentially important molecular target for cancer therapy. Reflecting the many mechanisms that seem to regulate survivin expression, diverse approaches have been evaluated for targeting survivin in experimental models. Although certain drugs, such as inhibitors of histone deacetylases,

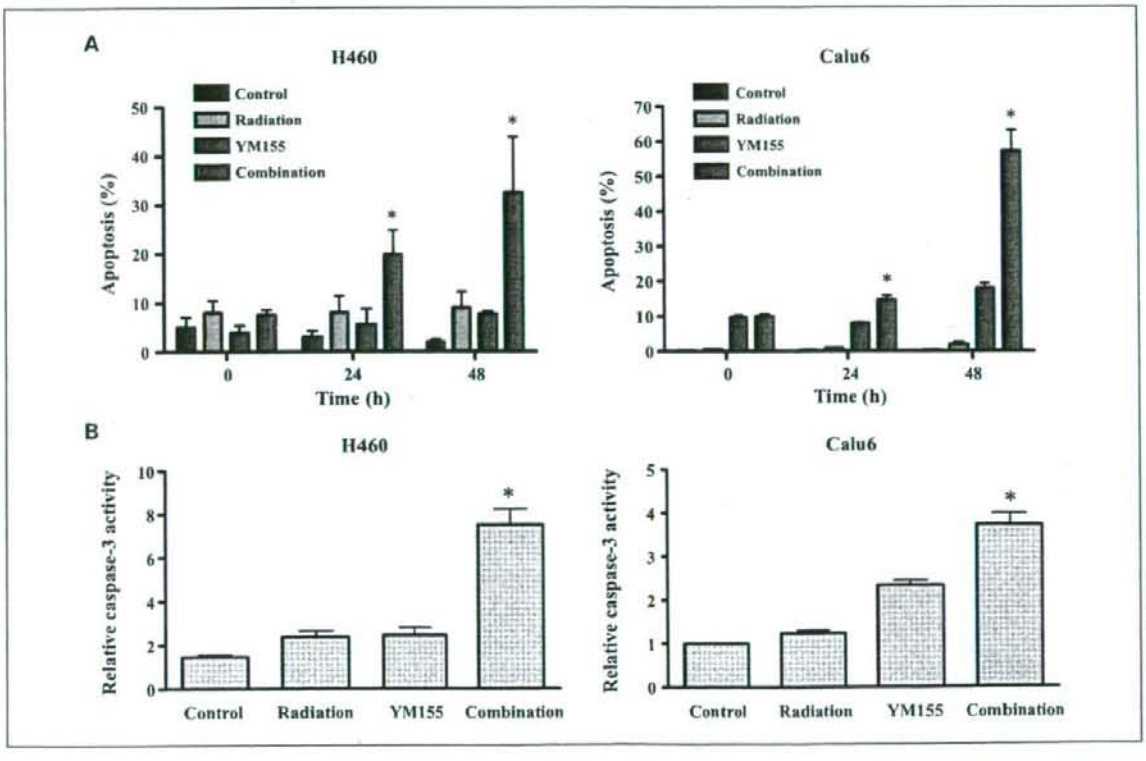

Fig. 3. Effect of YM155 on radiation-induced apoptosis and caspase-3 activity in H460 or Calu6 cells. *A*, cells were incubated with 50 nmol/L YM155 or vehicle (0.1% DMSO) for 48 h, exposed (or not) to 3 Gy of γ-radiation, and then incubated in drug-free medium for 24 or 48 h, at which times the percentage of apoptotic cells was determined by TUNEL staining. *B*, lysates of cells treated as in *A* were assayed for caspase-3 activity 24 h after irradiation. Columns represent means from three independent experiments; bars represent SD; those in *B* are expressed relative to the corresponding value for the control condition. * $P < 0.01$ versus the corresponding value for treatment with radiation or YM155 alone.

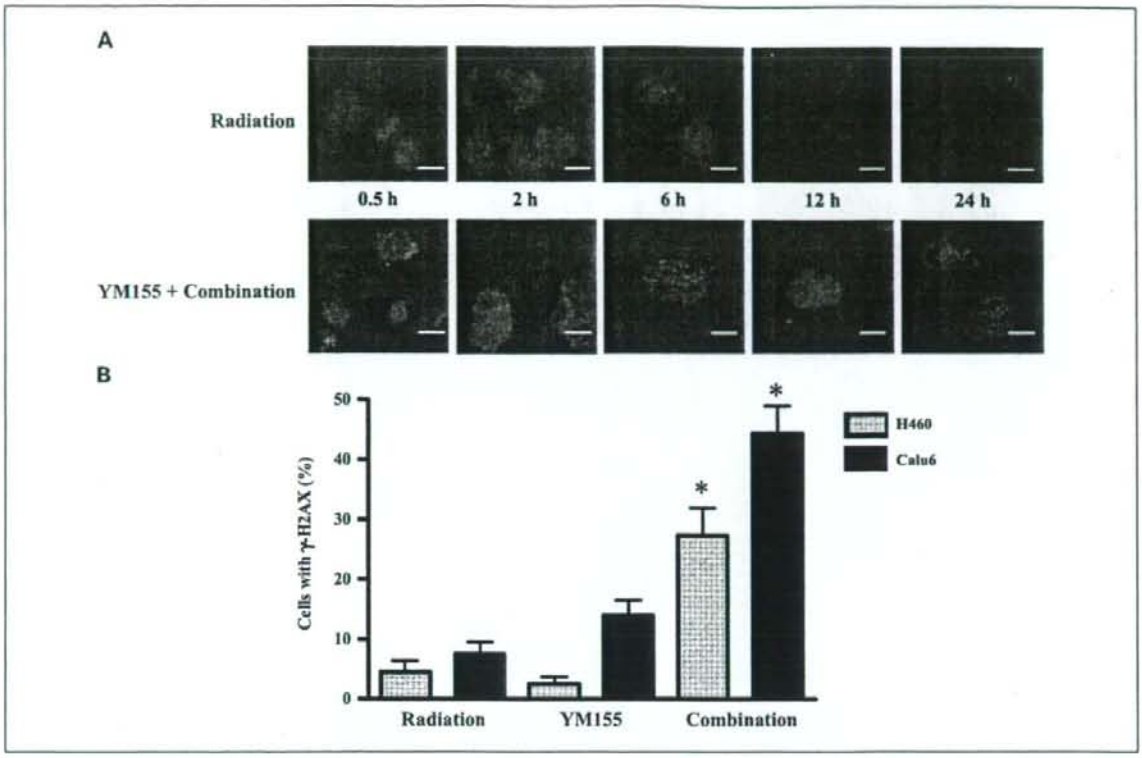

Fig. 4. Effect of YM155 on the radiation-induced formation of γ-H2AX foci in NSCLC cells. *A*, H460 cells were incubated with vehicle (0.1% DMSO) or 50 nmol/L YM155 for 48 h and then exposed to 3 Gy of γ-radiation. After incubation for the indicated times in drug-free medium, the cells were fixed and subjected to immunofluorescence staining for γ-H2AX (green fluorescence). Scale bar, 10 μm. *B*, H460 or Calu6 cells were incubated with vehicle or YM155 and then exposed (or not) to γ-radiation as in *A*. They were fixed at 24 h after irradiation and the percentage of cells containing γ-H2AX foci was determined. Columns represent means from three independent experiments; bars represent SD. $^*P < 0.05$ versus the corresponding value for radiation or YM155 alone.

mitogen-activated protein kinases, and cyclin-dependent kinases, have been shown to suppress survivin expression by targeting various signaling pathways, these drugs inhibit survivin expression nonspecifically (15–17, 19, 32). Gene therapy strategies based on small interfering RNA or other antisense oligonucleotides are specific for survivin, but the effective delivery of these molecules remains a challenge for the transition to the clinic (33). YM155 is a small-molecule agent that specifically inhibits survivin expression in various types of cancer cell lines *in vitro* (14). In addition, YM155 has been shown both to distribute preferentially to tumor tissues rather than to plasma as well as to exert pronounced antitumor activity in tumor xenograft models *in vivo* (14). The use of YM155 as a single agent in phase I clinical trials did not reveal significant toxicity (34). Although phase II studies of YM155 use as a single agent for certain types of cancer are currently under way, the effects of YM155 in combination with radiation have not been reported. We now show that YM155 increased the sensitivity of tumor cells to radiation *in vitro* and *in vivo*.

Clonogenic survival analysis, the most reliable approach for assessing the ability of genotoxic agents to induce cell death (35), revealed that YM155 markedly potentiated the decrease in NSCLC cell survival induced by γ-radiation. Given that induction of apoptosis is a key mechanism of cytotoxicity for most antitumor agents, including γ-radiation, defects in apoptotic signaling may underlie resistance to such agents (36). Radiation-sensitive tumors undergo radiation-induced apoptosis *in vitro* more readily than do radiation-resistant tumors (37–40). Treatment with caspase inhibitors has been shown to protect tumor cells against radiation-induced apoptosis and to increase their radioresistance (21, 41, 42), suggesting that radiation-induced apoptosis is caspase-dependent and that caspases contribute to radiosensitivity. The antiapoptotic activity of survivin is mostly attributable to inhibition of the activation of downstream effectors of apoptosis such as caspase-3 and caspase-7 (25). We have now shown that radiosensitization of NSCLC cells by YM155 was associated with increases both in the activity of caspase-3 and in the proportion of apoptotic cells. Our findings thus suggest that YM155 sensitized tumor cells to radiation at least in part by enhancing radiation-induced apoptosis.

We examined further the mechanism by which YM155 induces radiosensitization. Survivin is essential for the proper execution of mitosis and cell division, with disruption of survivin expression resulting in cell division defects that can lead to polyploidy and the formation of multinucleated cells (43, 44). Although treatment with 50 nmol/L YM155 for 48 hours inhibited survivin expression in NSCLC cells, it

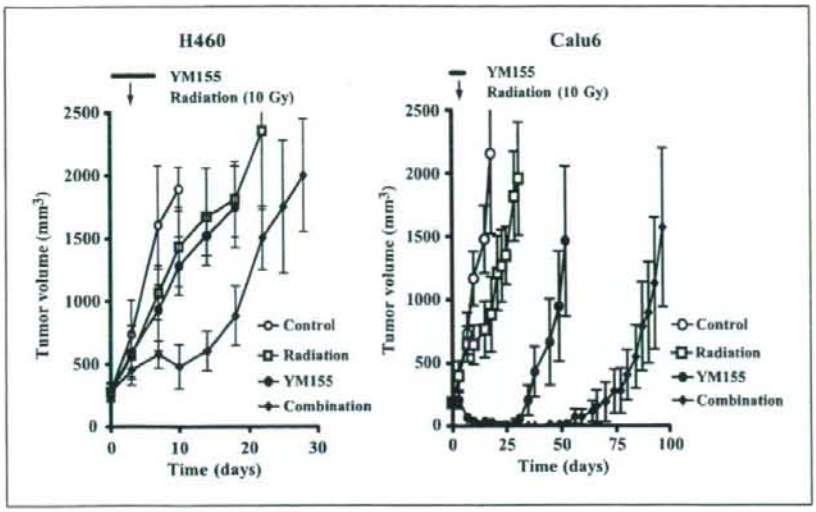

Fig. 5. Effect of YM155 on the growth of H460 or Calu6 tumors in mice subjected to single-dose radiotherapy. Cells were injected into the right hind limb of nude mice and allowed to grow. The mice were divided into four treatment groups: control, radiation alone, YM155 alone, or the combination of YM155 and radiation. YM155 (5 mg/kg) or vehicle was administered by continuous infusion over 7 d, and mice in the radiation groups were subjected to γ-irradiation with a single dose of 10 Gy on day 3 of drug treatment. Tumor volume was measured at the indicated times after the onset of treatment. Points, means from eight mice per group; bars, SE.

did not induce polyploidy (data not shown), suggesting that YM155-induced radiosensitization in the present study was not attributable to cell division defects caused by survivin depletion. Survivin was previously suggested to enhance tumor cell survival after radiation exposure through regulation of DSB repair (21). We therefore investigated the effect of YM155 on the repair of radiation-induced DSBs by immunofluorescence imaging of γ-H2AX foci. H2AX is a histone that is phosphorylated by ataxia telangiectasia mutated and DNA-dependent protein kinase in response to the generation of DSBs (45, 46). This reaction occurs rapidly, with half-maximal amounts of γ-H2AX generated within 1 minute and maximal amounts within 10 minutes (47), and a linear relation has been shown between the number of γ-H2AX foci and that of DSBs (48). The number of γ-H2AX foci is thus a sensitive and specific indicator of the existence of DSBs, with a decrease in this number reflecting DSB repair. We found that YM155 inhibited the repair of radiation-induced DSBs in NSCLC cells. If left unrepaired, DSBs can result in chromosome loss or cell death; agents that inhibit such repair thus increase the sensitivity of cells to ionizing radiation (49, 50). Our results therefore suggest that inhibition of DSB repair by YM155 contributes to the radiosensitization induced by this drug. Given that suppression of survivin expression impairs the repair of radiation-induced DNA damage (9, 21), our results further suggest that inhibition of DNA repair by YM155 is attributable to down-regulation of survivin expression.

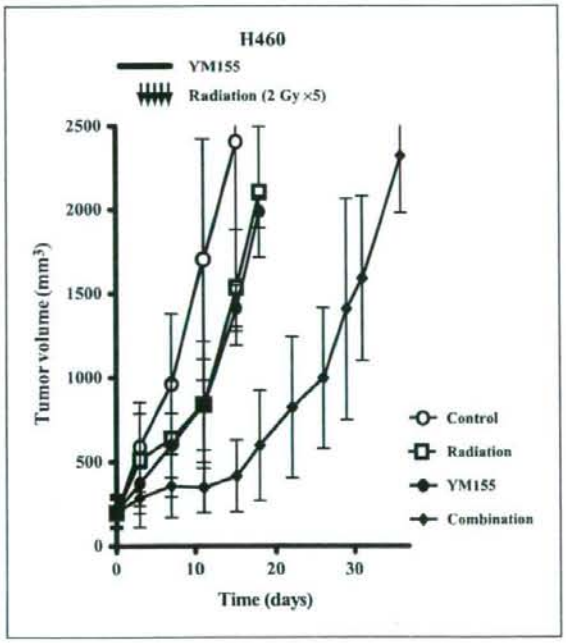

Fig. 6. Effect of YM155 on the growth of H460 tumors in mice subjected to fractionated radiotherapy. H460 cells were injected into the right hind limb of nude mice and allowed to grow. The mice were divided into four treatment groups: control, radiation alone, YM155 alone, or the combination of YM155 and radiation. YM155 (5 mg/kg) or vehicle was administered by continuous infusion over 7 d, and mice in the radiation groups were subjected to γ-irradiation with a daily dose of 2 Gy on days 3 to 7 of drug treatment. Tumor volume was measured at the indicated times after the onset of treatment. Points represent means from eight mice per group; bars represent SE.

The antitumor activity of YM155 has previously been shown to be time-dependent, with continuous infusion of the drug resulting in greater antitumor activity and less systemic toxicity compared with bolus injection in tumor xenograft models *in vivo* (14). Ongoing clinical trials of YM155 are thus being done with the drug administered on a continuous schedule. We also administered YM155 by continuous infusion in our *in vivo* experiments. The combination of YM155 with single-dose radiotherapy resulted in a marked increase in tumor growth delay compared with that apparent with either radiation or YM155 alone, indicating that YM155 enhanced the antitumor effect of ionizing radiation *in vivo*. Given that standard radiation therapy in the clinic is delivered according to a fractionated schedule, we also examined whether YM155 enhanced the tumor response to clinically relevant fractionated doses (2 Gy) of radiation. Indeed, YM155 was also effective in

British Journal of Cancer (2008) 99, 245–252

www.bjcancer.com

Mutations in the LKB1 tumour suppressor are frequently detected in tumours from Caucasian but not Asian lung cancer patients

JP Koivunen[1,2], J Kim[3,4], J Lee[3,4], AM Rogers[2], JO Park[1,2], X Zhao[2], K Naoki[2], I Okamoto[5], K Nakagawa[5], BY Yeap[6], M Meyerson[1,2,7,8,9], K-K Wong[1,2,9], WG Richards[10], DJ Sugarbaker[10], BE Johnson[1,2,9] and PA Jänne[*,1,2,9]

[1]*Lowe Center for Thoracic Oncology, Dana-Farber Cancer Institute, Boston, MA, USA;* [2]*Department of Medical Oncology, Dana-Farber Cancer Institute, Harvard Medical School, Boston, MA, USA;* [3]*Department of Thoracic Surgery, Samsung Medical Center, Seoul, Korea;* [4]*School of Medicine, Sungkyunkwan University, Seoul, Korea;* [5]*Department of Medical Oncology, School of Medicine, Kinki University, Osaka, Japan;* [6]*Department of Medicine, Massachusetts General Hospital, Boston, MA, USA;* [7]*Department of Pathology, Harvard Medical School, Boston, MA, USA;* [8]*The Broad Institute of MIT and Harvard Universities, Cambridge, MA, USA;* [9]*Department of Medicine, Brigham and Women's Hospital and Harvard Medical School, Boston, MA, USA;* [10]*Department of Surgery, Brigham and Women's Hospital, Boston, MA, USA*

Somatic mutations of *LKB1* tumour suppressor gene have been detected in human cancers including non-small cell lung cancer (NSCLC). The relationship between *LKB1* mutations and clinicopathological characteristics and other common oncogene mutations in NSCLC is inadequately described. In this study we evaluated tumour specimens from 310 patients with NSCLC including those with adenocarcinoma, adenosquamous carcinoma, and squamous cell carcinoma histologies. Tumours were obtained from patients of US ($n=143$) and Korean ($n=167$) origin and screened for *LKB1*, *KRAS*, *BRAF*, and *EGFR* mutations using RT—PCR-based SURVEYOR-WAVE method followed by Sanger sequencing. We detected mutations in the *LKB1* gene in 34 tumours (11%). *LKB1* mutation frequency was higher in NSCLC tumours of US origin (17%) compared with 5% in NSCLCs of Korean origin ($P=0.001$). They tended to occur more commonly in adenocarcinomas (13%) than in squamous cell carcinomas (5%) ($P=0.066$). *LKB1* mutations associated with smoking history ($P=0.007$) and *KRAS* mutations ($P=0.042$) were almost mutually exclusive with *EGFR* mutations ($P=0.002$). The outcome of stages I and II NSCLC patients treated with surgery alone did not significantly differ based on *LKB1* mutation status. Our study provides clinical and molecular characteristics of NSCLC, which harbour *LKB1* mutations.
British Journal of Cancer (2008) **99,** 245–252. doi:10.1038/sj.bjc.6604469 www.bjcancer.com
Published online 1 July 2008

Keywords: carcinoma; non-small cell lung; mutation; LKB1; EGFR; KRAS

Peutz–Jeghers syndrome (PJS) is caused by mutations in the *LKB1* tumour suppressor gene (Hemminki *et al*, 1998). LKB1 is serine–threonine kinase, which has been shown to regulate cell cycle progression, apoptosis, and cell polarity (Tiainen *et al*, 1999). The major target of LKB1 kinase activity is thought to be AMP-activated protein kinase (AMPK). AMPK is activated under low cellular energy conditions by raising AMP levels and it phosphorylates multiple downstream targets including tuberosclerosis complex 2 gene, which represses mTOR signalling. Phosphorylation of AMPK by LKB1 is needed for full activity of AMPK and suppression of mTOR activity under low energy conditions (Shaw *et al*, 2004). The hallmarks of PJS include mucocutaneous pigmentation and hamartomatous polyps of the gastrointestinal tract. Patients with PJS have an increased risk of developing gastrointestinal, pancreatic, breast, gynecological, and non-small cell lung cancers (NSCLC). The overall risk for cancers is increased 5- to 12-fold in different age groups compared with the general population (Hearle *et al*, 2006). Somatic mutations of the *LKB1* tumour suppressor have rarely been found in cancers from patients who do not have PJS except for NSCLC (Avizienyte *et al*, 1999). Previous reports have suggested the *LKB1* mutation rate to be as high as 30% in NSCLC tumours and cell lines derived from patients of Caucasian origin (Carretero *et al*, 2004; Matsumoto *et al*, 2007) and to be infrequent in NSCLC patients of Asian origin (3%) (Onozato *et al*, 2007). Furthermore, *LKB1* mutations have been shown to be associated with adenocarcinoma histology, male gender, and smoking history (Matsumoto *et al*, 2007). A recent report of using a mouse model for *lkb1* inactivation in NSCLC has provided insights into the role of the gene in this cancer. This study showed that *lkb1* inactivation in combination with activating mutations of *kras* using inducible promoters in the lung was associated with decreased survival compared with *kras* mutation alone (Ji *et al*, 2007).

Current screening techniques for *LKB1* tumour suppressor mutations rely on conventional exonic sequencing of the DNA, which can identify single base pair changes and small deletions/insertions (Ballhausen and Gunther, 2003). The addition of multiple ligation-dependent probe amplification (MLPA), which enables detection of exonic and whole gene deletions, with exonic sequencing has increased the mutation detection rates to 80% in patients with PJS phenotype (Volikos *et al*, 2006). Conventional

*Correspondence: Dr PA Jänne, Lowe Center for Thoracic Oncology, Dana-Farber Cancer Institute, D820A, 44 Binney Street, Boston, MA 02115, USA; E-mail: pjanne@partners.org
Revised 9 May 2008; accepted 28 May 2008; published online 1 July 2008

sequencing has also been used to detect mutations of *LKB1* at mRNA level and some mutations missed by sequencing at the DNA level have been discovered by mRNA-based approaches (Abed *et al*, 2001). However, mutant forms of *LKB1* mRNAs can have a shortened half-life because of nonsense-mediated decay, which can potentially interfere with mutation detection (Abed *et al*, 2001).

We have recently described a rapid and sensitive enzymatic method to detect mutations in epidermal growth factor (*EGFR*) of DNA from fresh tissue and paraffin-embedded tissues (Janne *et al*, 2006). This method includes amplification of region of interest with PCR, SURVEYOR endonuclease digestion of the products, which cleaves mismatched heteroduplex DNAs, and detection of DNA fragments by sensitive high-performance liquid chromatography (HPLC) WAVE HS system. Subsequently, SURVEYOR-positive specimens are fractionated in partially denaturing conditions and are Sanger-sequenced. The major advantages of SURVEYOR-WAVE method are the fast exclusion of wild-type specimens without laborious conventional sequencing and high sensitivity. The SURVEYOR-WAVE method is more sensitive than conventional sequencing as it can detect mutant DNA sequences when they are present in 1% or more of total DNA (Janne *et al*, 2006).

The current study was designed to analyse the incidence of *LKB1* mutations in NSCLC. Furthermore, we wanted to investigate the *LKB1* mutational frequency in different histologies and ethnic backgrounds, and assess their correlation to smoking history, gender, stage, survival, and other oncogenic mutations in NSCLC.

MATERIALS AND METHODS

Cell lines and tumour specimens

The NSCLC cell lines A549, NCI-H1395, NCI-H1650, NCI-H1666, NCI-H1781, NCI-1975, NCI-H23, NCI-H2126, NCI-H441, NCI-H820, HCC2935, HCC4006, and HCC827 were purchased from ATCC (Manassas, VA, USA). H3255, H3255GR, HCC2279, and PC-9 have been previously described (Ono *et al*, 2004; Tracy *et al*, 2004; Engelman *et al*, 2006). Ma1, and Ma70 are NSCLC cell lines harbouring *EGFR* mutations that were established at the Kinki University, Osaka, Japan. A549, NCI-H1395, NCI-H1666, NCI-H23, NCI-H2122, NCI-H2126, and NCI-H460 have previously been reported to contain *LKB1* mutations (Sanchez-Cespedes *et al*, 2002; Bamford *et al*, 2004; Carretero *et al*, 2004).

NSCLC tumours ($n=310$) were collected from surgical resections from patients with stages I–IV NSCLC when sufficient material for RNA extraction was available. The majority of the specimens ($n=167$) was collected at the Samsung Medical Center, Seoul, Korea. Frozen tumour tissues were collected from 809 out of 2442 patients who underwent curative resection for NSCLC from November 1995 to February 2007 at Samsung Medical Center. One or two pieces from the periphery of the tumour masses – avoiding necrotic regions – were immediately frozen at −80°C until retrieved. Medical records and haematoxylin and eosin-stained slides of the specimen were reviewed by a single pathologist. Only frozen tumour tissues from adenocarcinoma or squamous cell carcinoma (according to the 2004 World Health Organization histopathological criteria) were included. Only frozen tumour tissues with a tumour cell content of more than 70% were used for further analysis. In addition, frozen tumour tissues of the following patients were excluded from the study: patients who had received preoperative neoadjuvant treatments, patients with double primary lung cancer, and patients who had undergone incomplete resections or who had not been subjected to mediastinal lymph node dissections. Selected frozen tumour tissues were used for the microdissection. Briefly, frozen tissues were lightly stained with haematoxylin–eosin to improve visualisation, and necrotic tumour tissues and intervening normal tissues were removed. Each of the microdissected tumour tissues with a tumour cell content of more than 90% was placed in 1 ml Easy Blue reagent of a commercially available RNA isolation kit (easy-spin™ Total RNA Extraction Kit, iNtRON Biotechnology, Gyeonggi-do, Korea), immediately homogenised by vortexing, and the total RNA was extracted. The quantity and quality of RNA were analysed using a spectrometer (Nanodrop Technologies, Rockland, DE, USA) and Agilent 2100 Bioanalyzer (Agilent RNA 6000 Nano Kit, Agilent Technologies Inc., Böblingen, Germany), respectively. Finally, 167 frozen tissues with acceptable quality of RNA (RNA Integrity Number (RIN) value over 7.0) were used for the current studies. All patients provided written informed consent.

The tumours from Caucasian patients ($n=143$) were collected at the Brigham and Women's Hospital, Boston, MA, USA between 1991 and 1997 and have been previously published for patient characteristics and histology, and for expression profile-based clustering of the tumours (Bhattacharjee *et al*, 2001; Hayes *et al*, 2006). Frozen samples of resected lung tumours were obtained within 30 min of resection and subdivided into 100 mg samples and snap frozen at −80°C. Each specimen was associated with an immediately adjacent sample embedded for histology in an optimal cutting temperature medium and stored at −80°C. Six micrometres of frozen sections of embedded samples stained with haematoxylin and eosin were used to confirm the postoperative pathological diagnosis and to estimate the cellular composition of adjacent samples. All specimens underwent pathological review by two pathologists. In all 109 tumours obtained during the same time period were excluded because they did not meet one or more of the eligibility criteria. Tissue samples were homogenised in Trizol (Life Technologies, Gaithersburg, MD, USA) and RNA was extracted and purified by using the RNeasy column purification kit (Qiagen, Chatsworth, CA, USA). Denaturing formaldehyde gel electrophoresis followed by northern blotting using a β-actin probe assessed RNA integrity. Samples were excluded if β-actin was not full length. All patients provided written informed consent. The US cohort included specimens that have previously undergone analyses and the results have been published for *EGFR*, *KRAS*, and *BRAF* mutations (Bhattacharjee *et al*, 2001; Naoki *et al*, 2002; Hayes *et al*, 2006). We reconfirmed the mutations in 30 of these specimens using the SURVEYOR-based analysis (see section SURVEYOR digestion and HPLC analysis) and found 100% concordance between the two methods (data not shown).

Cell line specimens were snap frozen and stored at −80°C. RNA was extracted from tumours and cell lines using Trizol (Invitrogen, Carlsbad, CA, USA), purified with Rneasy Mini Kit (Qiagen, Valencia, CA, USA) and was used for cDNA synthesis using the QuantiTect reverse transcription kit (Qiagen, Valencia, CA, USA).

PCR primers and cycling conditions

For *LKB1* gene analysis, PCR primers were designed to amplify the cDNA in two amplicons. PCR primers of the first amplicon were designed to hybridise to the noncoding area of the mRNA upstream of exon 1 (5′-agggaagtcggaacacaagg-3′) and to exon 5 (5′-ccagatgtccaccttgaagc-3′) generating a PCR product of 797 bp. The primers for the second amplicon located at exon 5 (5′-aacggcc tggacaccttct-3′) and to noncoding exon 10 (5′-gaaccggcaggaagact gag-3′) generating a product of 702 bp, which has an overlapping part with first amplicon. For SURVEYOR-WAVE analysis of *KRAS*, PCR primers (5′-ggcctgctgaaaatgactga-3′, 5′-tcctgagcctgttttgtgtct-3′) were designed to generate an amplicon of 407 bp covering codons 12, 13 and 61, which are the codons commonly mutated in lung cancers. For SURVEYOR-WAVE mutation analysis of *BRAF*, cDNA was amplified in two overlapping amplicons (5′-aggattt cgtggtgatggag-3′, 5′-gatgacttctggtgccatcc-3′, and 5′-gacgggactcgagt gatgat-3′, 5′-ggtatcctcgtcccaccata-3′) covering codons 387–673. For SURVEYOR-WAVE analysis of *EGFR*, PCR amplification was done in a single amplicon (5′-ggagcctcttacacccagtg-3′,

5′-aggtcatcaactcccaaacg-3′), which covered exons 18–21 of the gene. PCR amplification was done using JumpStart Taq (Sigma, St Louis, MO, USA) under the manufacturer's guidelines. A part of the specimens ($n=103$) was previously characterised for *KRAS*, *BRAF*, *EGFR* mutations using reverse transcritase (RT)–PCR and direct sequencing of the PCR products (Naoki *et al*, 2002; Hayes *et al*, 2006).

SURVEYOR digestion and HPLC analysis

SURVEYOR digestion and HPLC analysis were carried out as described previously (Janne *et al*, 2006). In brief, PCR products were digested in reaction mixture containing equal volumes of SURVEYOR enzyme (Transgenomics, Omaha, NE, USA) and Enhancer (Transgenomics, Omaha, NE, USA) at 42°C for 20 min followed by termination of the reaction by Stop Solution (Transgenomics, Omaha, NE, USA). Specimens were then loaded to the WAVE HS HPLC (Transgenomics, Omaha, NE, USA) at 50°C, eluted with an increasing acetonitrile gradient, and detected by UV detector using DNA intercalating fluorescence dye (Transgenomics, Omaha, NE, USA). When cell lines known to be homozygous for specific mutation were analysed, PCR products were mixed 1:1 with PCR products of a wild-type cell line, denatured by heating, and slowly renatured to generate heteroduplexes.

Sequencing and fractionation

Specimens that showed an altered pattern on the SURVEYOR tracings were purified using QIAquick kit (Qiagen, Valencia, CA, USA) and sequenced bi-directionally by molecular biology core facility of Dana–Farber Cancer Institute. If a specimen showed an altered pattern on the SURVEYOR tracing but had a wild-type sequence by direct DNA sequencing, it underwent fractionation by WAVE HS HPLC in partially denaturing conditions. Running temperatures for specific amplicons were calculated by the Navigator Software (Transgenomics, Omaha, NE, USA). Collected fragments were amplified with PCR using the same primers as in the original amplification, purified and sequenced as previously described above.

Statistical analysis

Fisher's exact test was used to assess the association of *LKB1* mutation status with other clinical, pathological, and genetic characteristics. To adjust for any difference between ethnic groups, the association between *LKB1* mutation rate and each characteristic was also evaluated as stratified contingency tables. If we did not reject that the odds ratios were the same across ethnic groups, we then tested whether the common odds ratios were unity based on the stratified Mantel–Haenszel estimate (Breslow and Day, 1980). Overall survival was estimated using the Kaplan–Meier method, with differences between the groups compared using the log-rank test. All *P*-values were based on a two-sided hypothesis, with $P<0.05$ considered to be statistically significant and $0.05<P<0.10$ considered to be borderline significant.

RESULTS

SURVEYOR-WAVE mutation detection of *LKB1* tumour suppressor in NSCLC cell lines

The impact of the stability of *LKB1* mRNA on detecting *LKB1* mutations was tested using RT–PCR with mRNA extracted from NSCLC cell lines that had previously been characterised for *LKB1* mutations. These included NCI-H441 (wild type) and A549, NCI-H1395, NCI-H23, and NCI-H2126 (all containing *LKB1* mutations). Reverse transcriptase–PCR amplification of the whole coding region of the *LKB1* mRNA showed that cell lines with nonsense (A549, NCI-H23) mutations or 1 bp deletion (H1395) expressed mRNA with comparable size to the wild-type H441 cell line (1460 bp). H2126 cell line, which is known to have homozygous deletion of exons 4–6, expressed mRNA with substantially smaller size (~1000 bp) corresponding to deletion of 398 bp. RT–PCR revealed no major difference in *LKB1* mRNA expression levels between *LKB1* mutant or wild-type cell lines (Figure 1A).

As *LKB1* mutant and wild-type cell lines expressed comparable amounts of *LKB1* mRNA with RT–PCR, we studied the cDNA for mutations using the SURVEYOR-WAVE method. The WAVE HPLC provides a system to analyse DNA fragments smaller than 900 bp and therefore we designed two overlapping amplicons covering exons 1–5 (797 bp) and 5–9 (702 bp) to amplify the whole coding region of *LKB1* mRNA. PCR products of *LKB1* mutant cell lines were mixed 1:1 with the products from wild-type cell lines (H441) to generate heteroduplexes as *LKB1* mutant cell lines were previously reported to be homozygous for the inactivation of the gene. SURVEYOR-WAVE analysis of the amplicon covering exons 1–5 revealed novel peaks with the cDNA for A549, and NCI-H1395 cell lines compared with the wild type from NCI-H441 (Figure 1B). SURVEYOR-WAVE analysis of exons 5–9 showed novel peaks for the NCI-H23 cell line as well. The mutations detected with SURVEOR-WAVE were confirmed by conventional DNA sequencing and they corresponded to previous reports (Sanchez-Cespedes *et al*, 2002; Carretero *et al*, 2004). We could not detect the *LKB1* mutation of H2126 cell line with SURVEYOR-WAVE method using a two-amplicon approach because this cell line has a homozygous deletion of exons 4–6 and the reverse primer of the first amplicon and the forward primer of the second amplicon, which lie on the deleted part of the gene (data not shown).

LKB1 tumour suppressor gene mutations in NSCLC tumours

We next used the SURVEYOR-WAVE method to screen NSCLC tumour specimens ($n=310$) for *LKB1* mutations. We detected 34 *LKB1* mutations (11%) in the NSCLC tumour specimens (Table 1). The majority of the *LKB1* mutations detected was deletions or insertions ($n=25$, 74%). The remainder was missense ($n=7$, 21%) and nonsense ($n=2$, 6%) mutations (Table 2, Figure 1C). About one-half of the deletions and insertions were small, covering <15 bp ($n=14$, 56%), whereas larger deletions ($n=11$, 44%) covering hundreds of base pairs were detected in the remaining specimens. Some mutational hotspots were discovered. The areas that had the same mutation in more than one tumour specimen included deletion of exon 4 ($n=4$), deletion of exons 2 and 3 ($n=3$), D194Y ($n=2$), and P281L ($n=2$). Interestingly, a significant portion of the mutations was located in exon 1 ($n=11$, 32%) but there was no area of recurrent mutations in this exon (Table 2). Of the missense mutations detected in the current study, all except R426W are in the kinase domain of the protein. Missense mutations in codons 176 and 194 have been previously characterised in PJS (Launonen, 2005). We also found four F354L alterations (data not shown) but we did not consider these as missense mutations as this alteration has previously been reported to be a rare polymorphism of the gene (Launonen *et al*, 2000). We did not have access to the corresponding normal tissues and therefore, we could not verify if some of the missense mutations were somatic or germline.

Association of *LKB1* tumour suppressor mutations in NSCLC with clinicopathological characteristics

The mutation frequency of *LKB1* gene was significantly higher in NSCLCs in the Caucasian cohort (Table 1). Twenty-five (17% of specimens) of the *LKB1* mutations were detected in NSCLCs

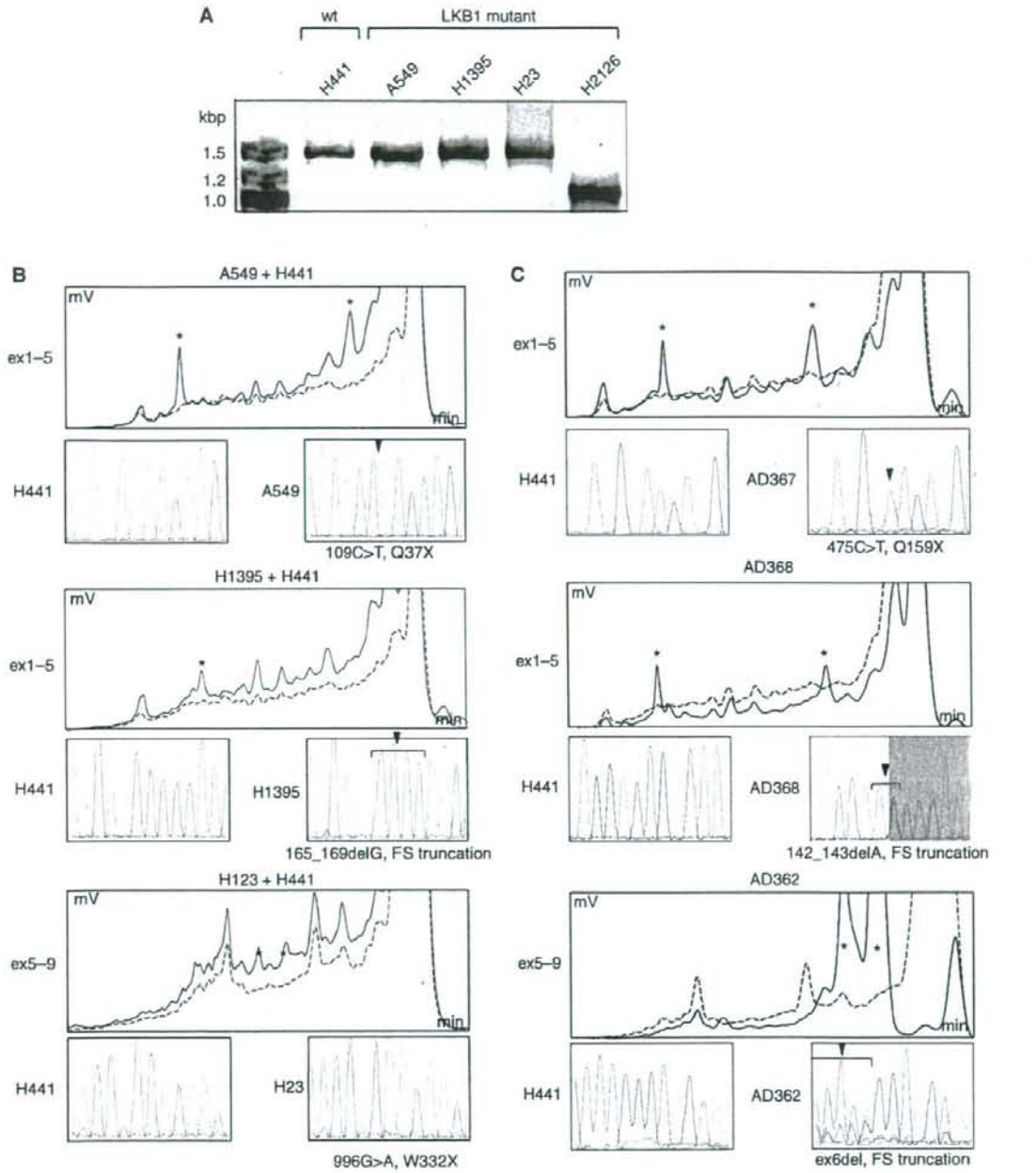

Figure 1 Mutation analysis of *LKB1* gene in NSCLC cell lines and tumours. RT–PCR amplification of cDNA from *LKB1* wt (H441) and *LKB1* mutant (A549, H1395, and H23) cell lines display the full length LKB1 mRNA (1.4 kbp) while the *LKB1* mutant cell line, H2126 with a deletion of exons 4–6 expresses a shorter mRNA (1.0 kbp) (**A**). HPLC tracings of SURVEYOR-WAVE mutation analysis of NSCLC cell lines A549, H1395, or H23 (continuous line), and H441 (dashed line). Time in minutes is shown on the *X*-axis, voltage in mV on the *Y*-axis (**B**). A549 and H1395 show novel peaks (*) in the amplicon covering exons 1–5 (ex1–5) corresponding to 109C>T, Q37X and 165_169delG, frameshift and truncation (FS truncation) mutations. The analysis from H23 demonstrates novel peaks in the amplicon covering exons 5–9 (ex5–9) corresponding to 996G>T, W332X mutation. *LKB1* wild-type cDNA (H441) was added to PCR products 1 : 1, denatured by heating and slowly renaturated to generate heteroduplexes since A549, H1395, and H23 have previously reported to be homozygous for the *LKB1* mutations. SURVEYOR-WAVE mutation analyses of NSCLC tumours (**C**). AD367 and AD368 tumours showed novel peaks in the ex1–5 amplicon corresponding to 475C>T, Q159X, and 142_143delA, FS, truncation mutations. AD362 tumour had novel peaks in ex5–9 amplicon corresponding to deletion of exon 6. Mutant sequences for AD367 and AD368 are displayed from sequences using the forward primer while mutation of the AD362 is showed with reverse primer.

Table 1 Frequency of *LKB1* mutations in NSCLC tumours and their association with clinicopathological characteristics

	LKB1 mutation		
	+	–	P-value*
All tumours	34 (11%)	276 (89%)	
Age, median	61.2	62.2	
Ethnicity			
Caucasian cohort	25 (17%)	118 (83%)	0.001
Asian cohort	9 (5%)	158 (95%)	
Gender			
Male	20 (11%)	167 (89%)	NS
Female	14 (12%)	107 (88%)	
Smoking			
Never (<10 py)	2 (3%)	70 (97%)	0.007
Smoker (>10 py)	26 (14%)	161 (86%)	
Tumour stage			
I	19 (10%)	169 (90%)	NS
II	8 (14%)	51 (86%)	
III	5 (11%)	42 (89%)	
IV	1 (12%)	7 (88%)	
Histology			
Adenocarcinoma	27 (13%)	180 (87%)	0.047
Squamous carcinoma	5 (5%)	87 (95%)	
Adenosquamous	2 (22%)	7 (78%)	

*Fisher's exact test, NS = not statistically significant ($P>0.05$).

collected from patients in the United States, whereas only nine mutations (5% of specimens) were detected in the Korean cohort ($P=0.001$) (Table 1). The *LKB1* mutation rate tended to be higher in adenocarcinomas (13%) compared with squamous cell carcinomas (5%) ($P=0.067$). Differences in histological subgroups were relatively modest in the US cohort with mutations in 18 out of 94 (19%) adenocarcinomas *vs* 5 out of 38 (13%) in squamous cell cancers ($P=0.461$). This is in contrast to the findings in the Asian patients where all of the *LKB1* mutations were detected in adenocarcinomas (9 out of 113 (8%)) and none were detected in squamous cell cancers (0 out of 54 (0%); $P=0.032$). Nevertheless, the higher rate of *LKB1* mutation in adenocarcinomas compared with squamous cell carcinomas retains the same level of statistical significance (stratified $P=0.064$) after adjusting for fluctuation between ethnic groups. The US cohort also included nine specimens from adenosquamous carcinomas and two out of nine (22%) had *LKB1* mutations, which is similar to the frequency in adenocarcinomas in this population (Table 1). There was no association between *LKB1* mutations and the clinical stage of the NSCLC patients. Kaplan–Meier survival curves of stages I and II NSCLC patients showed a tendency for shorter survival in patients with *LKB1* mutant tumours but this, however, did not reach statistical significance ($P=0.17$) (Figure 2). No differences in survival were observed in patients who harboured both *LKB1* and *KRAS* mutations compared with those with *KRAS* or *LKB1* alone but the total number of patients with both mutations who had stages I or II NSCLC was small ($n=9$; data not shown). We detected an association of *LKB1* mutations with a smoking history ($P=0.007$) and only two mutations were detected in tumours from 72 NSCLC patients who were either never or light (≤10 pack years) former smokers (Table 1). After adjusting for ethnic group, the higher rate of *LKB1* mutation among patients with a smoking history is borderline significant (stratified $P=0.067$). The reduction in statistical significance is likely owing to the loss of power associated with the overall rarity of *LKB1* mutations among never or light former smokers. For these analyses we combined both never smokers and light (≤10 pack years) smokers as the frequency of mutations in other oncogenes such as *EGFR* is similar in these two patient groups (Pham *et al*, 2006). There were no correlations between *LKB1* mutations and gender or age of a patient.

Table 2 The specific *LKB1* mutations in NSCLC tumours

Mutation type	No. (%)	Mutation	Amino acid change	Exon	Histology
Missense	7 (21)	*526G>T	D176Y	4	Ad
		*580G>T	D194Y	4	Ad
		580G>T	D194Y	4	Sq
		829G>T	D277Y	6	AdSq
		*842C>T	P281L	6	Ad
		*842C>T	P281L	6	Ad
		1276C>T	R426W	9	Ad
Nonsense	2 (6)	206C>A	S69X	1	Ad
		475C>T	Q159X	4	Ad
Deletion/ insertion	25 (74)	*75_76del2&insT	FS, truncates	1	Ad
		120_130del11	FS, truncates	1	Ad
		125_127insGG	FS, truncates	1	Ad
		128_129delC	FS, truncates	1	Ad
		142_143delA	FS, truncates	1	Ad
		180delC	FS, truncates	1	Ad
		209delA	FS, truncates	1	Ad
		227_228delC	FS, truncates	1	Ad
		47_651del604	FS, truncates	1-5	Sq
		153_536del384	FS, truncates	1-4	AdSq
		*exon 2-3del	Truncates	2-3	Sq
		*exon 2-3del	Truncates	2-3	Ad
		exon 2-3del	Truncates	2-3	Ad
		exon 2-4del	FS, truncates	2-4	Sq
		464_465del2insTTTGCT	FS, truncates	3-4	Sq
		562_563delG	FS, truncates	4	Ad
		*exon 4del	FS, truncates	4	Ad
		exon 4del	FS, truncates	4	Ad
		exon 4del	FS, truncates	4	Ad
		exon 4del	FS, truncates	4	Ad
		610_623del14	FS, truncates	5	Ad
		*837_844delC	FS, truncates	6	Ad
		837_844insC	FS, truncates	6	Ad
		exon 6del	FS, truncates	6	Ad
		1038_1040insG	FS, truncates	8	Ad

Ad = Adenocarcinoma; AdSq = Adenosquamous carcinoma; Sq = Squamous cell carcinoma; . *These mutations were detected in Korean NSCLC patients.

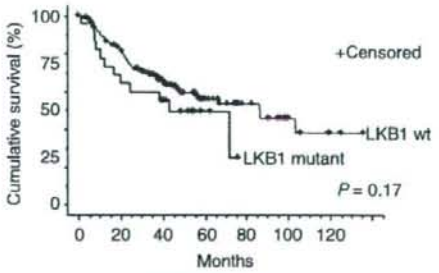

Figure 2 Kaplan–Meyer survival curves of stage I and II NSCLC patients with LKB1 wildtype (red line, $n=198$) *vs* LKB1 mutant (blue line, $n=23$) tumours.

Association of *LKB1* mutations with *K-Ras*, *B-Raf*, and *EGFR* mutations in NSCLC

Previous reports have suggested that in NSCLC cell lines, *LKB1* mutations often occur concurrently with *KRAS* or *BRAF* mutations

(Sanchez-Cespedes *et al*, 2002; Carretero *et al*, 2004). Furthermore, *EGFR* mutations are often mutually exclusive with *KRAS* mutations in NSCLC (Kosaka *et al*, 2004; Marchetti *et al*, 2005). We used combined data from previous papers (Sanchez-Cespedes *et al*, 2002; Carretero *et al*, 2004) and from Sanger institute's databases (Bamford *et al*, 2004) to analyse association of *LKB1* mutations with mutations of *KRAS*, *BRAF*, and *EGFR*. Analysis of *LKB1* mutation harbouring NSCLC cell lines (A-427, A549, NCI-H1395, NCI-H1666, NCI-H2122, NCI-H2126, NCI-H23, and NCI-H460) showed that five of the cell lines (63%) had concurrent *LKB1* and *KRAS* mutations, two (25%) had concurrent *LKB1* and *BRAF* mutations, and only one (13%) had neither *KRAS* nor *BRAF* mutations. None of these cell lines had EGFR mutations.

As our findings in NSCLC cell lines suggested concurrency of *KRAS* or *BRAF* and mutual exclusiveness of *EGFR* mutations with LKB1 mutations, we analysed the mutational status of these genes in our primary NSCLC tumour specimens. *KRAS* mutations were detected in 49 (16% in the whole tumour set, 25% in Caucasian and 8% in Asian specimens) tumour specimens with 10 (20% of *KRAS* mutants) of these occurring concurrently with an *LKB1* mutation ($P = 0.042$) (Table 3). Four *BRAF* mutations (1%) were found in the tumour set (G465V, N581S, L596R, and T599I) and one of these (N581S) occurred concurrently with *LKB1* mutation ($P = 0.373$). Seventy tumours (23% in the whole tumour set, 9% in Caucasian, 34% in Asian specimens) had *EGFR* kinase domain mutations with only one of them occurring concurrently with an *LKB1* mutation ($P = 0.002$). The tumour with a concurrent *EGFR* and *LKB1* mutation had a missense mutation of *LKB1* outside the kinase domain (R426W). No germ line DNA was available from this patient. However, a recent report has suggested that R426W is in fact a rare polymorphism of the gene (Onozato *et al*, 2007). Taken together our findings suggest that unlike *KRAS*, mutations in *EGFR* and *LKB1* are mutually exclusive in NSCLC.

Previous reports (Sanchez-Cespedes *et al*, 2002; Carretero *et al*, 2004) and Cancer Genome Project by Sanger Institute (Bamford *et al*, 2004) have extensively characterised *LKB1* mutations in NSCLC cell lines with *KRAS* and *BRAF* mutations, but *LKB1* status of *EGFR* mutant NSCLC cell lines has not been extensively analysed. Therefore, we analysed the *LKB1* genotype of NSCLC cell lines with known *EGFR* or *ERBB2* mutations. Twelve *EGFR* mutant and one *ERBB2* mutant cell lines were analysed for *LKB1* genotype. No *LKB1* mutations were detected in these cell lines (Table 4).

Table 3 Association of *LKB1* mutations with *KRAS*, *BRAF*, and *EGFR* mutations in NSCLC tumours

		LKB1 mutation		
		+	−	P-value*
EGFR mutation	+	1	69	0.002
	−	33	207	
K-Ras mutation	+	10	39	0.042
	−	24	237	
B-Raf *mutation*	+	1	3	0.373
	−	33	273	

*Fisher's exact test.

Table 4 LKB1 genotypes of NSCLC cell lines with EGFR or ERBB2 mutations

Cell line	*EGFR* genotype	*HER2* genotype	*LKB1* genotype
H1650	E746_A750del	Wt	Wt
H1781	Wt	G776V, Cins	Wt
H1975	L858R, T790M	Wt	Wt
H3255	L858R	Wt	Wt
H3255GR	L858R, T790M	Wt	Wt
H820	L747_L751del, T790M	Wt	Wt
HCC2279	E746_A750del	Wt	Wt
HCC2935	E746_T751del, S752I	Wt	Wt
HCC4006	L747_E749del, A750P	Wt	Wt
HCC827	E746_A750del	Wt	Wt
Ma-1	E746_A750del	Wt	Wt
Ma-70	L858R	Wt	Wt
PC-9	E746_A750del	Wt	Wt

Wt = wild type.

DISCUSSION

The present study characterised *LKB1* mutation frequency in NSCLC using one of the largest tumour sets to date ($n = 310$). Our study analysed tumours from different histologies and of both a US and Korean origin to determine potential histological and ethnic variation in *LKB1* mutational frequency. The large size of our study enabled us to study associations of *LKB1* mutations with clinocopathological factors, which have been incompletely characterised in previous studies (Sanchez-Cespedes *et al*, 2002; Carretero *et al*, 2004; Fernandez *et al*, 2004; Matsumoto *et al*, 2007; Onozato *et al*, 2007). In addition, we used a modification of a sensitive mutation screening technique that we have previously developed to facilitate the rapid detection of *LKB1* mutations (Janne *et al*, 2006).

Findings from our study confirm the high frequency of *LKB1* mutations in NSCLC (11%), which in contrast, are rare (0–4%) in other common solid malignancies (Avizienyte *et al*, 1998, 1999). The reason behind these observations is presently unknown but might reflect the differences in carcinogen exposure in the lungs compared with other tissues. In support of this hypothesis, we find that *LKB1* mutations are significantly ($P = 0.007$) more common in smokers than in never or light ($\leqslant 10$ pack years) cigarette smokers (Table 1). Male PJS patients (age $\geqslant 50$ years) have an increased risk of developing lung cancer compared with the general population but the relationship of smoking and the increased risk of lung cancer in PJS is unknown (Hearle *et al*, 2006). Interestingly, the *LKB1* mutation spectrum found in the current study is very similar to those previously published for PJS (deletions 34%, insertions 15%, splice site mutations 14%, missense mutations 21%, and nonsense mutations 12%) (Launonen, 2005) and, as in PJS, no clear mutational hotspots were detected.

Our study also demonstrated that the *LKB1* mutation frequency was significantly higher in cancers derived from a US population compared with those found in Korean patients (17 *vs* 5%; $P = 0.001$). These differences also track with cigarette smoking, as the number of never/light former smokers was much higher in the Korean cohort compared with the US cohort of patients (38 *vs* 13%). Similarly, a recent study of 100 Japanese NSCLCs found that only 3% contained an *LKB1* mutation (Onozato *et al*, 2007). These findings are in contrast to *EGFR* mutations, which are more frequently detected in tumours from never/light cigarette smokers and from Asian patients (Janne and Johnson, 2006). Our studies further highlight ethnic and environmental differences in the origins of NSCLC.

Given the differences in *LKB1* mutation frequencies in smokers *vs* never/light smokers and in the US compared with Korean patients, we further determined whether these were also associated with other oncogene mutations known to vary in these subgroups of patients. Consistent with prior studies we found a significant association with concurrent *KRAS* mutations, which are common in smokers (Ahrendt *et al*, 2001), in one out of three of NSCLC with *LKB1* mutations (Table 3). In contrast, there was a significant inverse relationship of *LKB1* mutations with *EGFR* mutations in both NSCLC tumours and cell lines, which has not previously been

described (Tables 3 and 4). These differences may relate to the biological role of LKB1 in lung cancer. It is possible that in *EGFR* mutant lung cancers there is already maximal activation of the PI3K/Akt/mTOR signalling pathway and thus an *LKB1* mutation may not be required to further potentiate this signalling pathway. In contrast in *KRAS* mutant cancers, a concurrent *LKB1* mutation may be required to enhance mTOR activation. Mice with concurrent *KRAS* mutations and *LKB1* inactivation have more aggressive tumours and a shorter survival than those with only *KRAS* mutant cancers (Ji *et al*, 2007). In our study, we were not able to detect a significant survival difference for patients whose tumours contained *LKB1* mutations alone or concurrently with *KRAS* mutations (data not shown) likely because of the limited number of tumour specimens. Additional studies are needed to clarify the prognostic impact of *LKB1* mutations in humans with NSCLC. In the present study ~2 out of 3 of *LKB1* mutant tumours were *KRAS* wild type (Table 3). One possibility is that such tumours contain a concurrent mutation in another oncogene that activates the same signalling pathway as *KRAS*. For this reason, we examined our tumours for *BRAF* mutations, which are found in 1–2% of NSCLC (Naoki *et al*, 2002). We detected a concurrent *LKB1* mutation in one of the four *BRAF* mutant tumours (Table 3). This tumour was wild type for *KRAS* (data not shown). In addition, some of the *BRAF* mutant NSCLC cell lines (NCI-H1395, G469A; NCI-H1666, G466V) also contain a concurrent *LKB1* mutation (Sanchez-Cespedes *et al*, 2002; Bamford *et al*, 2004; Carretero *et al*, 2004). Future studies will help further clarify whether *LKB1* mutations occur concurrently with other genomic alterations in NSCLC and the impact of this on patient outcome.

Our study employed a mutation scanning technology to screen for *LKB1* mutations at the cDNA level (Janne *et al*, 2006). This was advantageous as the entire coding region of *LKB1* could be rapidly screened for a mutation using just two overlapping cDNA fragments. *LKB1* is a challenging gene to analyse at the genomic DNA level because of its high guanine–cytosine content. In addition, as many of the *LKB1* mutations are small deletions (Table 2) or involve deletions of entire exons, these would be missed using exon-specific genome sequencing methods. Our method, however, does have limitations as it would miss deletions at the site of PCR primers, whole gene deletions, or deletions within the promoter region all of which have been infrequently detected in PJS (Volikos *et al*, 2006). Thus our studies may underestimate the true *LKB1* mutation frequency in NSCLC. In addition, our method is limited to the analysis of fresh tumour specimens, which are available only from the minority of NSCLC patients. Furthermore, as techniques isolating mRNA from formalin-fixed paraffin-embedded tumour specimens continue to improve, this rapid mutation scanning technique can be used to analyse broader populations of tumours from NSCLC patients. Future studies may need to employ a combination of *LKB1* mutation detection methodologies including the current method, MLPA and direct sequencing.

ACKNOWLEDGEMENTS

This study is supported by grants from the National Institutes of Health 1RO1CA114465-01 (BYY, BEJ, and PAJ), the National Cancer Institute Lung SPORE P20CA90578-02 (BYY and BEJ), American Cancer Society RSG-06-102-01-CCE (BYY and PAJ), Finnish Medical Foundation (JPK), Finnish Cultural Foundation (JPK), and Academy of Finland (JPK). PAJ, MM, and BEJ are part of a pending patent application on *EGFR* mutations.

REFERENCES

Abed AA, Gunther K, Kraus C, Hohenberger W, Ballhausen WG (2001) Mutation screening at the RNA level of the STK11/LKB1 gene in Peutz-Jeghers syndrome reveals complex splicing abnormalities and a novel mRNA isoform (STK11 c.597(insertion mark)598insIVS4). *Hum Mutat* **18:** 397–410

Ahrendt SA, Decker PA, Alawi EA, Zhu Yr YR, Sanchez-Cespedes M, Yang SC, Haasler GB, Kajdacsy-Balla A, Demeure MJ, Sidransky D (2001) Cigarette smoking is strongly associated with mutation of the K-ras gene in patients with primary adenocarcinoma of the lung. *Cancer* **92:** 1525–1530

Avizienyte E, Loukola A, Roth S, Hemminki A, Tarkkanen M, Salovaara R, Arola J, Butzow R, Husgafvel-Pursiainen K, Kokkola A, Jarvinen H, Aaltonen LA (1999) LKB1 somatic mutations in sporadic tumors. *Am J Pathol* **154:** 677–681

Avizienyte E, Roth S, Loukola A, Hemminki A, Lothe RA, Stenwig AE, Fossa SD, Salovaara R, Aaltonen LA (1998) Somatic mutations in LKB1 are rare in sporadic colorectal and testicular tumors. *Cancer Res* **58:** 2087–2090

Ballhausen WG, Gunther K (2003) Genetic screening for Peutz-Jeghers syndrome. *Expert Rev Mol Diagn* **3:** 471–479

Bamford S, Dawson E, Forbes S, Clements J, Pettett R, Dogan A, Flanagan A, Teague J, Futreal PA, Stratton MR, Wooster R (2004) The COSMIC (Catalogue of Somatic Mutations in Cancer) database and website. *Br J Cancer* **91:** 355–358

Bhattacharjee A, Richards WG, Staunton J, Li C, Monti S, Vasa P, Ladd C, Beheshti J, Bueno R, Gillette M, Loda M, Weber G, Mark EJ, Lander ES, Wong W, Johnson BE, Golub TR, Sugarbaker DJ, Meyerson M (2001) Classification of human lung carcinomas by mRNA expression profiling reveals distinct adenocarcinoma subclasses. *Proc Natl Acad Sci USA* **98:** 13790–13795

Breslow NE, Day NE, International Agency for Research on Cancer (1980) Statistical methods in cancer research. Vol. 1. Analysis of case–control studies. IARC scientific publications; no. 32. International Agency for Research on Cancer: Lyon

Carretero J, Medina PP, Pio R, Montuenga LM, Sanchez-Cespedes M (2004) Novel and natural knockout lung cancer cell lines for the LKB1/STK11 tumor suppressor gene. *Oncogene* **23:** 4037–4040

Engelman JA, Mukohara T, Zejnullahu K, Lifshits E, Borras AM, Gale CM, Naumov GN, Yeap BY, Jarrell E, Sun J, Tracy S, Zhao X, Heymach JV, Johnson BE, Cantley LC, Janne PA (2006) Allelic dilution obscures detection of a biologically significant resistance mutation in EGFR-amplified lung cancer. *J Clin Invest* **116:** 2695–2706

Fernandez P, Carretero J, Medina PP, Jimenez AI, Rodriguez-Perales S, Paz MF, Cigudosa JC, Esteller M, Lombardia L, Morente M, Sanchez-Verde L, Sotelo T, Sanchez-Cespedes M (2004) Distinctive gene expression of human lung adenocarcinomas carrying LKB1 mutations. *Oncogene* **23:** 5084–5091

Hayes DN, Monti S, Parmigiani G, Gilks CB, Naoki K, Bhattacharjee A, Socinski MA, Perou C, Meyerson M (2006) Gene expression profiling reveals reproducible human lung adenocarcinoma subtypes in multiple independent patient cohorts. *J Clin Oncol* **24:** 5079–5090

Hearle N, Schumacher V, Menko FH, Olschwang S, Boardman LA, Gille JJ, Keller JJ, Westerman AM, Scott RJ, Lim W, Trimbath JD, Giardiello FM, Gruber SB, Offerhaus GJ, de Rooij FW, Wilson JH, Hansmann A, Moslein G, Royer-Pokora B, Vogel T, Phillips RK, Spigelman AD, Houlston RS (2006) Frequency and spectrum of cancers in the Peutz-Jeghers syndrome. *Clin Cancer Res* **12:** 3209–3215

Hemminki A, Markie D, Tomlinson I, Avizienyte E, Roth S, Loukola A, Bignell G, Warren W, Aminoff M, Hoglund P, Jarvinen H, Kristo P, Pelin K, Ridanpaa M, Salovaara R, Toro T, Bodmer W, Olschwang S, Olsen AS, Stratton MR, de la Chapelle A, Aaltonen LA (1998) A serine/threonine kinase gene defective in Peutz-Jeghers syndrome. *Nature* **391:** 184–187

Janne PA, Borras AM, Kuang Y, Rogers AM, Joshi VA, Liyanage H, Lindeman N, Lee JC, Halmos B, Maher EA, Distel RJ, Meyerson M, Johnson BE (2006) A rapid and sensitive enzymatic method for epidermal growth factor receptor mutation screening. *Clin Cancer Res* **12:** 751–758